doi:10.1093/plcell/koab165

THE PLANT CELL

THE PLANT CELL 2021: 33: 3004–3021

Research Article

HBI transcription factor-mediated ROS homeostasis regulates nitrate signal transduction

Xiaoqian Chu [1], Jia-Gang Wang [1,2], Mingzhe Li [1], Shujuan Zhang [3], Yangyang Gao [4], Min Fan [1], Chao Han [1], Fengning Xiang [1], Genying Li [3], Yong Wang [4], Xiang Yu [5], Cheng-Bin Xiang [6] and Ming-Yi Bai [1,*,†]

1 The Key Laboratory of Plant Development and Environmental Adaptation Biology, Ministry of Education, School of Life Sciences, Shandong University, Qingdao 266237, China
2 College of Agriculture, Shanxi Agricultural University, Taigu 030801, China
3 Crop Research Institute, Shandong Academy of Agricultural Sciences, Jinan 250100, China
4 State Key Laboratory of Crop Biology, College of Life Sciences, Shandong Agricultural University, Tai'an 271018, China
5 School of Life Sciences & Biotechnology, Shanghai Jiao Tong University, Shanghai 200240, China
6 School of Life Sciences and Division of Molecular & Cell Biophysics, Hefei National Science Center for Physical Sciences at the Microscale, University of Science and Technology of China, Hefei 230027, China

*Author for correspondence: baimingyi@sdu.edu.cn
†Senior author.

These authors contributed equally to this work (X.C., J-G.W).

X.C., J.W., and M.B. together designed the experiments. X.C. performed the statistical analysis of plant growth, transient expression. X.C., J.W., and X.Y. performed the RNA-Seq and GO analysis. J.W. performed the western blot, subcellular location analysis, and ChIP–qPCR. M.L., C.H., M.F., S.Z., Y.G., X.C., and J.W. generated HBI1-related mutants, *HBI1-Ox/cat2cat3* and *NLP7-YFP/cat2cat3* transgenic plants. G.L., F.X., Y.W., and C.X. provided the critical discussion on the work. X.C. and J.W. performed all other experiments. X.C., J.W., and M. B. wrote the manuscript.

The author responsible for distribution of materials integral to the findings presented in this article in accordance with the policy described in the Instructions for Authors (https://academic.oup.com/plcell) is: Ming-Yi Bai (baimingyi@sdu.edu.cn).

Abstract

Nitrate is both an important nutrient and a critical signaling molecule that regulates plant metabolism, growth, and development. Although several components of the nitrate signaling pathway have been identified, the molecular mechanism of nitrate signaling remains unclear. Here, we showed that the growth-related transcription factors HOMOLOG OF BRASSINOSTEROID ENHANCED EXPRESSION2 INTERACTING WITH IBH1 (HBI1) and its three closest homologs (HBIs) positively regulate nitrate signaling in *Arabidopsis thaliana*. HBI1 is rapidly induced by nitrate through NLP6 and NLP7, which are master regulators of nitrate signaling. Mutations in *HBIs* result in the reduced effects of nitrate on plant growth and ~22% nitrate-responsive genes no longer to be regulated by nitrate. HBIs increase the expression levels of a set of antioxidant genes to reduce the accumulation of reactive oxygen species (ROS) in plants. Nitrate treatment induces the nuclear localization of NLP7, whereas such promoting effects of nitrate are significantly impaired in the *hbi-q* and *cat2 cat3* mutants, which accumulate high levels of H_2O_2. These results demonstrate that HBI-mediated ROS homeostasis regulates nitrate signal transduction through modulating the nucleocytoplasmic shuttling of NLP7. Overall, our findings reveal that nitrate treatment reduces the accumulation of H_2O_2, and H_2O_2 inhibits nitrate signaling, thereby forming a feedback regulatory loop to regulate plant growth and development.

Received January 26, 2021. Accepted June 09, 2021. Advance access publication June 15, 2021

IN A NUTSHELL

Background: Nitrate is both an essential macronutrient for plants and a critical signaling molecule that regulates plant metabolism, growth, and crop yield. Reactive oxygen species (ROS), as the by-products of aerobic metabolism, initially studied in relation to their damaging effects, have emerged as major regulators of plant growth and development, as well as plant responses to stress. Deprivation of nitrogen triggers the accumulation of ROS. The inhibition of ROS accumulation by chemical agents blocked the induction of gene expression associated with the nitrate-starvation response. However, the interplay between nitrate and ROS signaling in plant development remains unclear.

Question: Do ROS affect the nitrate signal transduction in plants? We tested this by analyzing nitrate-regulated gene expression and plant growth in the presence or absence of ROS.

Findings: We found that the growth-related transcription factor HBI1 is rapidly induced by nitrate through NLP6 and NLP7, which are master regulators of nitrate signaling pathway. HBI1 increases the expression levels of a set of antioxidant genes to reduce the ROS in plants. Treatment with hydrogen peroxide (H_2O_2), an important ROS signaling molecule, suppresses the nitrate-stimulated plant growth and downstream gene expression. Nitrate supply induces the nuclear localization of NLP7, whereas such promoting effects of nitrate are significantly impaired in mutants of *hbi-q* and *cat2 cat3* that accumulate high levels of ROS. Overall, our findings reveal that nitrate treatment reduces the accumulation of ROS, and ROS inhibits nitrate signaling, thereby forming a feedback regulatory loop to regulate plant growth and development.

Next steps: When plants are grown under the biotic or abiotic stress conditions, nitrate signaling is significantly inhibited and nitrogen use efficiency is reduced. Adequate regulation of the activity of key components in the nitrate signaling pathway will help to improve plant tolerance to different stress conditions.

Introduction

Nitrogen is an essential macronutrient for plants, and its availability is a key determinant of plant growth and development and crop yield (Xu et al., 2012; O'Brien et al., 2016; Wang et al., 2018b; Fredes et al., 2019; Vidal et al., 2020). Hence, nitrogen fertilizers have been used as the major driving force for the improvement of crop yield worldwide (Stitt, 1999; Crawford and Forde, 2002; Wang et al., 2018b; Vidal et al., 2020). Nitrate is the main form of nitrogen available in the soil for plant uptake. Moreover, nitrate serves as the nitrogen signal for the rapid induction of a transcriptional response, called the "primary nitrate response" (PNR), which regulates a wide range of developmental processes including seed germination, root architecture, shoot development, and flowering (Forde, 2014; Yan et al., 2016; Lin and Tsay, 2017; Gras et al., 2018; Landrein et al., 2018). Nitrate is sensed by the dual-affinity transceptor (transporter/receptor) NITRATE TRANSPORTER 1.1 (NRT1.1/CHL1/NPF6.3), which is a dual-affinity transporter and can switch between high and low affinities through phosphorylation and dephosphorylation at the Thr101 site in response to different nitrate concentrations (Ho et al., 2009). At low concentrations of nitrate, NRT1.1 is phosphorylated by CIPK23–CBL9 complex (CIPK, CALCINEURIN B-LIKE (CBL)-INTERACTION PROTEIN KINASE; CBL, CALCINEURIN B-LIKE PROTEIN), shifting into a high-affinity nitrate transporter. In contrast, at high nitrate levels, NRT1.1 is dephosphorylated and turns into a low-affinity transporter (Ho et al., 2009; Hu et al., 2009). Nitrate triggers the accumulation of calcium ions (Ca^{2+}) in the cytoplasm and nucleus, thereby activating three Ca^{2+}-SENSOR PROTEIN KINASES (CPKs), namely CPK10, CPK30, and CPK32, which phosphorylate the NIN-like protein Nin-Like Protein (NLP)7 to promote its nuclear localization, where it acts as a master transcription factor to regulate the expression of a subset of nitrate-responsive genes in *Arabidopsis thaliana* (Marchive et al., 2013; Liu et al., 2017; Alvarez et al., 2020).

Reactive oxygen species (ROS), as the by-products of aerobic metabolism, initially studied in relation to their damaging effects, have emerged as major regulators of normal plant growth and development, as well as plant responses to stress (Mittler, 2017; Waszczak et al., 2018). Under nitrogen deficiency conditions, ROS concentration increases in Arabidopsis roots, suggesting that root hair cells may contain a sensing system for nitrogen deprivation (Shin et al., 2005). Recent studies in Arabidopsis uncovered an important role of ROS in nitrogen demand and nitrogen-mediated signal transduction (Jung et al., 2018; Safi et al., 2018). Deprivation of nitrogen triggers the accumulation of hydrogen peroxide (H_2O_2), which functions as a versatile signaling modulator in various regulatory pathways. The inhibition of H_2O_2 accumulation by chemical agents, such as potassium iodide or diphenyleniodonium NADPH-oxidase inhibitor), blocked the induction of gene expression associated with the nitrogen-starvation response (Safi et al., 2018). In maize (*Zea mays*), nitrogen depletion or NO_3^- supply affects the balance between superoxide ($O_2^{\bullet -}$) and H_2O_2 in the root apex transition zone through the regulation of *Zmupb1* and *Zmprx112* transcription (Trevisan et al., 2019). These findings indicated that ROS plays critical roles in nitrogen signal transduction pathway. However, the

interplay between ROS and nitrogen signaling in plant development remains unclear.

HOMOLOG OF BRASSINOSTEROID-ENHANCED EXPRESSION2 INTERACTING WITH IBH1 (HBI1), a basic helix–loop–helix (bHLH) transcription factor, has been shown to function as a major hub in the central growth circuit of plants to regulate plant growth and immunity (Bai et al., 2012; Fan et al., 2014; Malinovsky et al., 2014; Wang et al., 2014, 2018a; Neuser et al., 2019; Cai et al., 2020). Growth-promoting signals, including dark, shade, high temperature, auxin, gibberellin, and brassinosteroids activate HBI1 at the post-transcriptional level to promote cell elongation through the BZR-ARF-PIF/DELLA (BAP/D) module coupled with a tripartite module of HLH and bHLH factors (Chaiwanon et al., 2016). In contrast, the pathogen *Pst DC3000* and flagellin inhibit the activity of HBI1 at transcriptional level to repress plant immunity (Fan et al., 2014). A recent study reported that HBI1 regulates the tradeoff between growth and immunity by controlling apoplastic ROS homeostasis through the different regulation of the genes encoding NADPH oxidase and peroxidase. HBI1 directly induces the expression of *RESPIRATORY BURST OXIDASE HOMOLOG C* (*RbohC*), but represses the transcript accumulation of *RbohA* to promote cell expansion during leaf growth (Neuser et al., 2019). In addition, HBI1 interacts with the transcription factor TCP20 to positively regulate the C-terminally Encoded Peptides (CEP)-mediated systemic nitrate acquisition (Chu et al., 2020).

In this study, we show that HBI1 positively regulates nitrate signal transduction through controlling ROS homeostasis in plants. Nitrate supply significantly induces *HBI1* and *BEE2* expressions through NLP6 and NLP7. HBI1 promotes ROS scavenging by directly regulating the expression of *CAT2*. Loss of functions of *HBI1*, *BEE2*, and another two closet homolog genes lead to ROS accumulation, the reduced promoting effects of nitrate on shoot growth and root development, and ∼22% of nitrate-responsive genes were no longer regulated by nitrate. Nitrate treatment induced the nuclear localization of NLP7, but such effects of nitrates were impaired in *hbi-q* and *cat2 cat3* mutants, which accumulated high levels of H_2O_2 in plants. Together, our study reveals that HBI-mediated ROS homeostasis regulates nitrate signaling by modulating the nucleocytoplasmic shuttling of NLP7.

Results

HBI1 and *BEE2* are induced by nitrate

We have previously reported that HBI1 integrates a wide range of environmental signals and endogenous programs to regulate plant growth and immunity (Bai et al., 2012; Fan et al., 2014; Chu et al., 2020). To further understand the function of HBI1 in plant growth and development, we performed gene-expression analysis of *HBI1* in Arabidopsis transcriptomic data and found that the expression of *HBI1* and its homolog gene *BEE2* was rapidly induced by nitrate. Integrative network bioinformatics identified HBI1 as a potential regulatory transcription factor in the nitrate response, ranking among the top five candidate regulatory genes in Arabidopsis (Alvarez et al., 2014). To test whether *HBI1* and *BEE2* are regulated by nitrate, we analyzed the expression levels of *HBI1* and *BEE2* upon nitrate treatment at different times or different concentrations. The transcript levels of *HBI1* and *BEE2* significantly increased as early as 15 min after nitrate treatment and increased over time (Figure 1A; Supplemental Figure S1A). When grown under different concentrations of nitrate, *HBI1* and *BEE2* expression increased at more than 300-μM nitrate concentration and became more prominent with increasing nitrate concentrations, indicating that nitrate induced the expression of *HBI1* and *BEE2* in a dose-dependent pattern (Figure 1B). The levels of HBI1-YFP protein expressed from the constitutive *35S* promoter did not change dramatically after nitrate treatment, whereas the level of HBI1-YFP protein derived from its endogenous *HBI1* promoter significantly increased upon nitrate treatment, confirming that nitrate regulated *HBI1* at the transcriptional level (Supplemental Figure S1, B and C). These results strongly indicated that *HBI1* and *BEE2* are the early responsive genes of nitrate signaling.

Due to the rapid increase in the transcription levels of *HBI1* and *BEE2* upon nitrate treatment, we speculated that the core transcription factors involved in nitrate signaling contribute to the transcriptional regulation of *HBI1* and *BEE2*. NLP6 and NLP7 have been reported to be the master transcription factors in the nitrate signaling pathway (Marchive et al., 2013; Liu et al., 2017; Alvarez et al., 2020). To test whether the regulation of *HBI1* and *BEE2* by nitrate is dependent on NLP6 and NLP7, we performed reverse transcription quantitative polymerase chain reaction (RT-qPCR) experiments using wild-type plants, *nlp7-1* and *nlp6-1 nlp7-1* with or without nitrate treatment. Nitrate significantly induced the expression of *HBI1* and *BEE2* in wild-type plants, while such effects of nitrate were dramatically reduced in *nlp7-1* and *nlp6-1 nlp7-1* mutants (Figure 1C). The expression levels of *HBI1* homologous genes, including *bHLH44*, *bHLH50*, *bHLH137*, and *bHLH62*, were significantly induced by nitrate supply in wild-type plants, but weakly induced in *nlp6-1 nlp7-1* mutants (Supplemental Figure S2, A–F). Protoplast transient gene-expression assays showed that co-expression of NLP7 increased the expression of the luciferase reporter driven by the *HBI1 or BEE2* promoters (Figure 1, D and E). The recent published chromatin immunoprecipitation sequencing data of NLP7 showed HBI1 is the target gene of NLP7 (Alvarez et al., 2020). Consistent with this, our chromatin immunoprecipitation–quantitative PCR (ChIP–qPCR) analysis confirmed that NLP7 directly bound to the promoters of *HBI1* and *BEE2* (Figure 1, F and G). These results indicated NLP6 and NLP7 play critical roles in the nitrate-induced expression of *HBI1* and *BEE2*.

HBI and its close homologs (HBIs) positively regulate nitrate-mediated plant growth

Because *HBI1* and *BEE2* are early nitrate-responsive genes, we wanted to determine whether HBI1 and BEE2 are

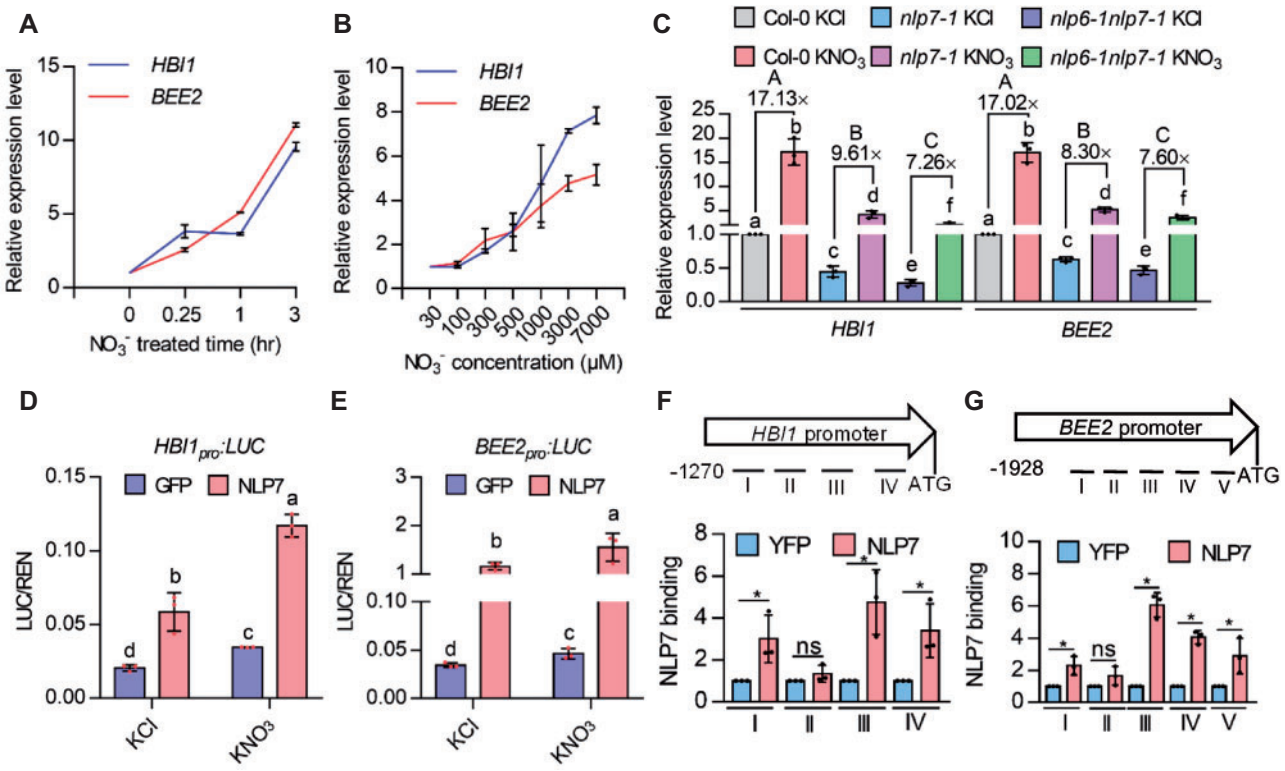

Figure 1 Nitrate induces the expression of *HBI1* and *BEE2*. A, *HBI1* and *BEE2* are the early responsive genes of nitrate. Seedlings of Col-0 grown on medium with 7-mM KNO_3 for 7 days were transferred to nitrogen-free medium for 2 days, and then treated with 10-mM KNO_3 for different times. B, Nitrate induces the expression of *HBI1* and *BEE2* in a dose-dependent manner. Wild-type (Col-0) plants were grown on medium containing different concentrations of KNO_3 for 14 days. The transcript levels of *HBI1* and *BEE2* were quantified by real-time PCR. *PP2A* gene was used as an internal control. Error bars are SD of three biological replicates. C, NLP6 and NLP7 play critical roles in the nitrate-induced expression of *HBI1* and *BEE2*. Seedlings of Col-0, *nlp7-1*, and *nlp6-1 nlp7-1* grown on medium with 7-mM KNO_3 for 7 days were transferred to nitrogen-free medium for 2 days, and then treated with 10-mM KNO_3 for 3 h. The transcript levels of *HBI1* and *BEE2* were quantified by real-time PCR. *PP2A* gene was used as an internal control. Error bars are SD of three biological replicates. Different letters above bars indicate statistically significant difference between samples (two-way ANOVA analysis followed by Tukey's test, $P < 0.05$). D, E, Transient gene expression assay showed NLP7 promoted the expression of *HBI1* and *BEE2*. The promoters of *HBI1 or BEE2* fused to the luciferase reporter gene were co-transfected with $35S_{pro}$*:GFP* or $35S_{pro}$*:NLP7-GFP* into mesophyll protoplast of wild-type plants with or without nitrate treatment. The luciferase activities were normalized by Renilla luciferase as an internal control. Different letters above bars indicate statistically significant difference between samples (two-way ANOVA analysis followed by Tukey's test, $P < 0.05$). F, G, ChIP-qPCR analysis of NLP7 binding to the promoters of *HBI1* and *BEE2*. The $35S_{pro}$*:NLP7-YFP* and $35S_{pro}$*:YFP* transgenic plants growing in half-strength Murashige and Skoog (MS) liquid medium for 12 days were used to perform the ChIP analysis. Schematic illustration of different regions in the promoters of *HBI1* and *BEE2*. The levels of NLP7 binding were calculated as the ratio between $35S_{pro}$*:NLP7-YFP* and $35S_{pro}$*:YFP* control, and then normalized to that of the control gene *PP2A*. Error bars indicate SD of three independent experiments. Asterisks between bars indicate statistically significant differences between samples (Student's *t* test, $^*P < 0.05$).

involved in nitrate-regulated plant growth and development. Nitrate has been reported to stimulate shoot growth and regulate the elongation of primary and lateral root (Araya et al., 2014; Moreno et al., 2020; Swift et al., 2020). We first analyzed the nitrate response in the loss-of-function mutants of *HBI1* and *BEE2*. The results showed *hbi1* and *bee2* single mutants displayed slightly decreased cotyledon size and fresh weight, and shorter primary and total lateral root lengths compared to wild-type plants in the presence of nitrate (Supplemental Figure S3, A–F). Considering the functional redundancy of HBI1 family, three closest genes of *HBI1* including *BEE2*, *bHLH31*, and *bHLH79* were selected to generate higher-order *HBI* mutants. The *hbi1 bee2* double mutants showed a significant reduction in cotyledon size, fresh weight, and root growth; the addition of mutations in *bHLH31* or *bHLH79* enhanced the phenotype of *hbi1 bee2*; and simultaneous mutation of *hbi1*, *bee2*, *bhlh31*, and *bhlh79* (*hbi-q*) resulted in significantly reducing the nitrate-promoting effects on plant growth. Overexpression of *HBI1* (*HBI1-Ox*) led to an enlarged cotyledon in all concentrations of nitrate and hypersensitivity to nitrate in terms of the promotion of plant fresh weight (Figure 2, A–C; Supplemental Figure S4, A and B). These results indicated that HBI1 and its homologs, which we termed HBIs, play important roles in nitrate-mediated plant growth and development.

To examine the functions of HBI1 in the nitrate-mediated plant growth and development, we analyzed the growth phenotypes of the wild-type Col-0, *hbi-q*, and *HBI1-Ox* that were grown in the medium containing the 7 mM different nitrogen sources under 16-h light/8-h dark photoperiod for

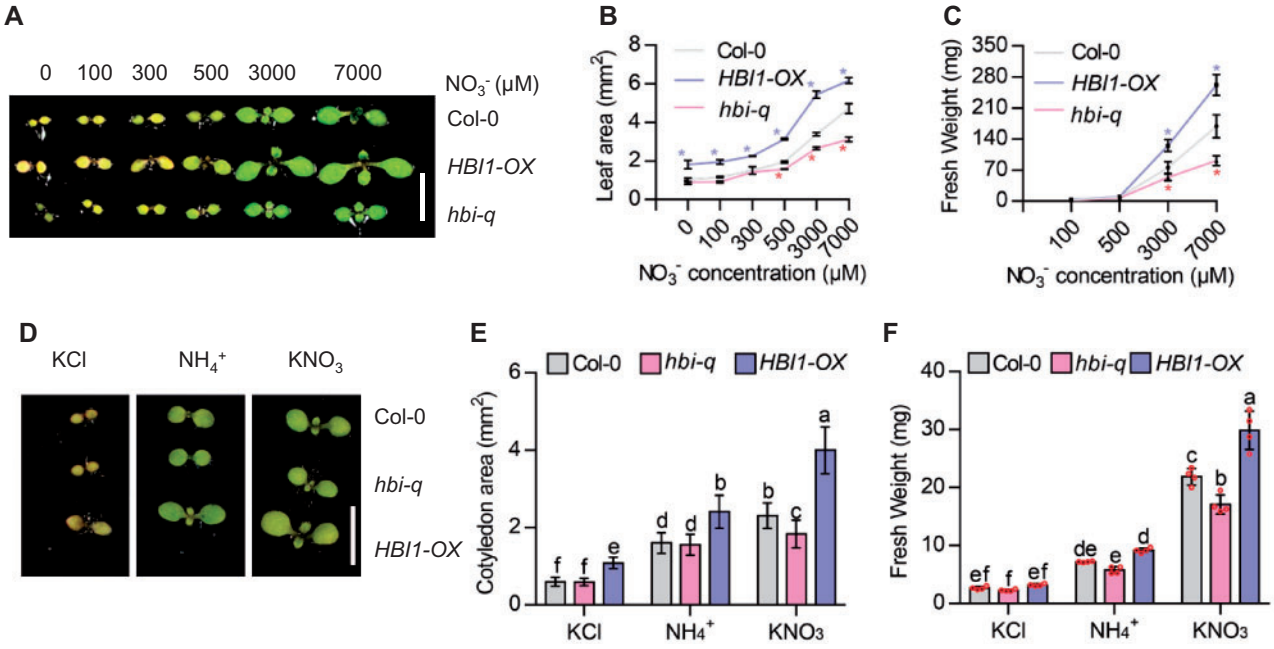

Figure 2 HBIs positively regulate nitrate-mediated plant growth. A, B, Quantification of HBI-stimulated shoot growth in the presence of different concentrations of nitrate. Seedlings of the wild-type, *HBI1-Ox*, and *hbi-q* were grown on the medium with different concentrations of nitrate for 7 days. Scale bar represents 5 mm. Error bars indicate SD (n = 16–30). Asterisks indicate statistically significant differences among Col-0, *HBI1-OX*, and *hbi-q* at individual nitrate concentration (Student's t test, *$P < 0.05$). C, Quantification of the fresh weight of the wild type, *HBI1-Ox*, and *hbi-q* that were grown on the medium with different concentrations of nitrate under 16-h light/8-h dark for 4 weeks. Error bars indicate SD (n = 15–26). Asterisks indicate statistically significant differences among Col-0, *HBI1-OX*, and *hbi-q* at individual nitrate concentration (Student's t test, *$P < 0.05$). D, E, Quantification of the promoting effects of HBIs on the shoot growth in the presence of different nitrogen sources. Seedlings of the wild-type, *HBI1-Ox*, and *hbi-q* were grown on the medium containing 7 mM different nitrogen sources for 7 days. Scale bar represents 5 mm. Error bars indicate SD (n = 20–36). Different letters above bars indicate statistically significant differences between samples (two-way ANOVA analysis followed by Tukey's test, $P < 0.05$). F, Quantification of the fresh weight of the wild-type, *HBI1-Ox*, and *hbi-q* that were grown on the medium with different nitrogen sources for 12 days. Every three plants is one group. Error bars indicate SD (n = 4). Different letters above bars indicate statistically significant differences between samples (two-way ANOVA analysis followed by Tukey's test, $P < 0.05$).

7 days. *HBI1-Ox* showed increased shoot growth and root development phenotype in all growth conditions (Figure 2, D–F). However, when plants were grown on medium containing KCl or NH_4^+, the *hbi-q* mutant displayed a similar growth phenotype to wild-type plants; and when plants were grown on the medium with KNO_3, nitrate significantly stimulated shoot growth in wild-type plants, but such effects of nitrate were significantly reduced in *hbi-q* (Figure 2, D–F). The *hbi-q* mutant exhibits deficiency in nitrate-regulated shoot growth and root development, indicating HBIs play important roles in the nitrate-mediated plant growth and development.

To further determine the functions of HBI1 in the nitrate signaling, we analyzed the shoot-growth phenotypes of the wild-type, *HBI1-Ox*, *chl1-5*, and *HBI1-Ox/chl1-5*. The results showed that *chl1-5* partially suppressed the promoting effects of HBI1 on shoot growth in the presence of nitrate (Supplemental Figure S5, A and B). These results suggested the promoting effects of HBI1 on plant growth are partial dependent on the nitrate transceptor CHL1/NRT1.1. Together, these results strongly demonstrated that HBIs play important roles in nitrate-promoted plant growth and development.

HBIs are required for nitrate-regulated gene expression

Given the important roles of HBIs in nitrate-mediated plant growth and the rapid induction of *HBIs* by nitrate, we speculated that HBIs are involved in the transcriptomic response to nitrate. To test this hypothesis, we carried out RNA sequencing (RNA-Seq) experiments with the wild-type Col-0, *hbi-q*, and *nlp7-1* plants that were grown on MGRL medium (7-mM nitrate) for 7 days, subjected to nitrate starvation 2 days, and then treated with 10-mM KCl or 10-mM KNO_3 for 3 h. RNA-Seq analysis identified 3,431, 3,703, and 3,541 differentially expressed genes (DEGs) that responded to nitrate in wild-type plants, *hbi-q*, and *nlp7-1* mutants, respectively (Figure 3, A and B; Supplemental Data Sets S1–S4), and they significantly overlapped with each other. Among the 3,431 genes regulated by nitrate in wild-type plants, 764 genes (22.3%) were no longer responsive to nitrate in *hbi-q* mutant, and 1,447 (42.2%) genes were not regulated by nitrate in the *nlp7-1* mutant. Of 764 HBI-affected nitrate-responsive genes, 604 genes (79.1%) also depended on NLP7 to respond to nitrate, indicating HBIs and NLP7 regulate the expression of nitrate-responsive genes through a common signaling pathway (Figure 3, A and B). Gene ontology (GO)

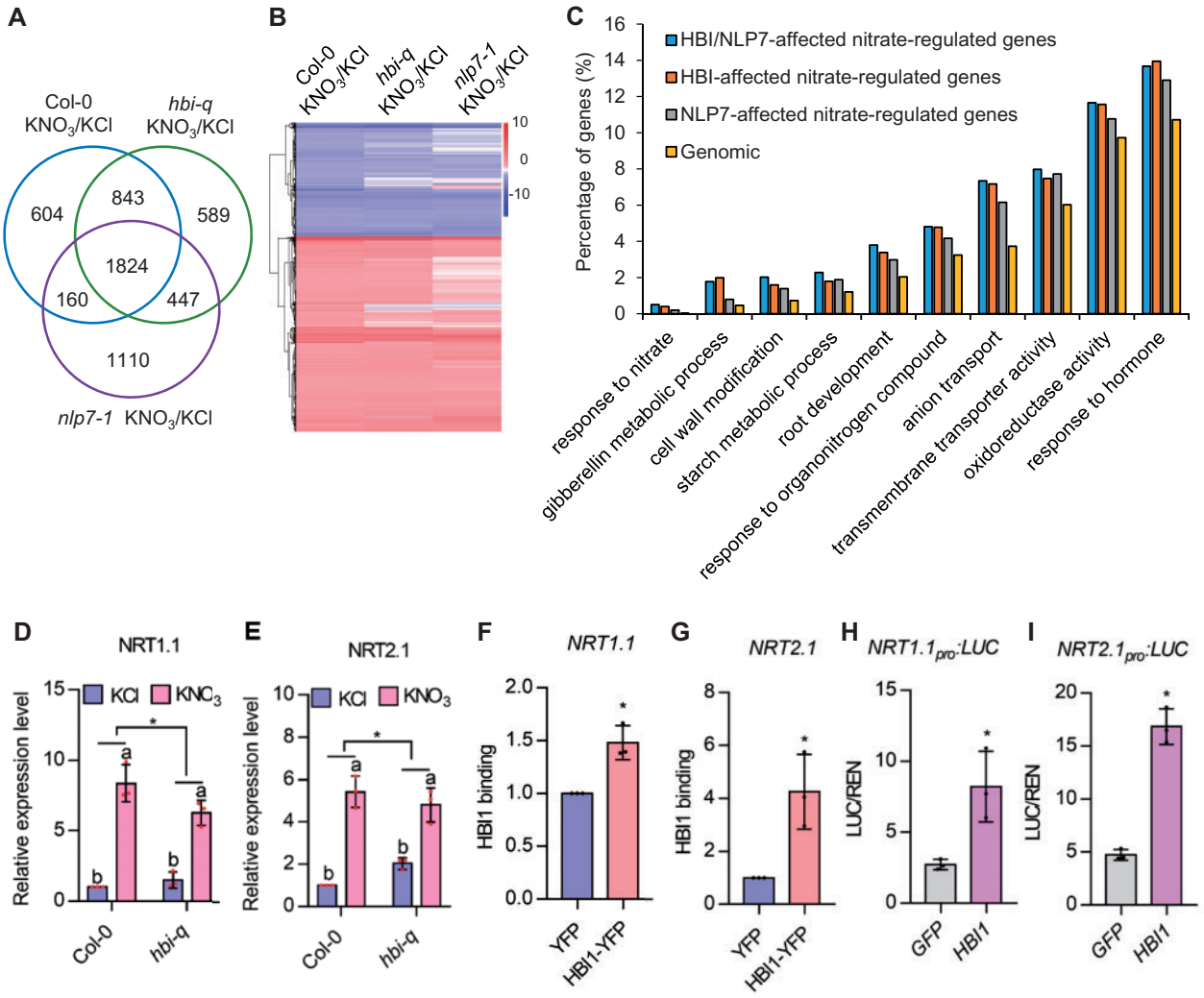

Figure 3 HBIs are required for nitrate-regulated gene expression. A, Venn diagram showing the overlap between sets of genes significantly regulated by nitrate in the wild-type, *nlp7-1*, and *hbi-q* mutants. B, Hierarchical cluster analysis of the expression data of 3,431 genes regulated by nitrate in the wild-type, *nlp7-1*, and *hbi-q*. The numerical values for the blue-to-red gradient bar represent $\log_2$ of the ratio. C, GO analysis of nitrate-regulated HBI1-affected, NLP7-affected, or HBI1- and NLP7 co-affected genes. Numbers indicate the percentages of genes belonging to each GO category. Genomic denotes the random genomic control. D, E, HBIs are required for nitrate-induced expression of *NRT1.1* and *NRT2.1*. Seedlings of Col-0 and *hbi-q* were grown on medium with 7-mM KNO_3 for 5 days, transferred to nitrogen-free medium for 2 days, and then treated with 10-mM KNO_3 for 30 min. The transcript levels of *NRT1.1* and *NRT2.1* were quantified by real-time PCR. *PP2A* gene was used as an internal control. Error bars are SD of three biological replicates. Different letters above bars indicate statistically significant differences between samples (two-way ANOVA analysis followed by Tukey's test, $P < 0.05$). Asterisks between bars indicate statistically significant different effects of nitrate on the expression of *NRT1.1* and *NRT2.1* in Col-0 and *hbi-q* (Student's *t* test, $^*P < 0.05$). F, G, HBI1 directly binds to the promoters of *NRT1.1* and *NRT2.1*. The $35S_{pro}$:*HBI1-YFP* and $35S_{pro}$:*YFP* transgenic plants growing in half-strength MS liquid medium for 12 days were used to perform the ChIP analysis. The levels of HBI1 binding were calculated as the ratio between $35S_{pro}$:*HBI1-YFP* and $35S_{pro}$:*YFP* control, and then normalized to that of the control gene *PP2A*. Error bars indicate SD of three independent experiments. Asterisks between bars indicate statistically significant differences between samples (Student's *t* test, $^*P < 0.05$). H, I, Transient assays showed that HBI1 induces the expression of *NRT1.1* and *NRT2.1*. The promoters of *NRT1.1* or *NRT2.1* fused to the luciferase reporter gene were co-transfected with $35S_{pro}$:*GFP* or $35S_{pro}$:*HBI-GFP* into mesophyll protoplasts of wild-type plants with or without nitrate treatment. The luciferase activities were normalized by Renilla luciferase as an internal control. Asterisks between bars indicate statistically significant differences between samples (Student's *t* test, $^*P < 0.05$).

analysis revealed that genes involved in nitrate and organonitrogen, transmembrane transporter, gibberellin metabolic, root development, and starch metabolism are the most significantly enriched functional classes of the HBI-affected nitrate-regulated genes and NLP7-affected nitrate-regulated genes, suggesting that HBIs, similar to NLP7, play important roles in diverse nitrate-mediated cellular and metabolic processes (Figure 3C).

To further determine the function of HBIs in nitrate-regulated gene expression, we performed the RT-qPCR to compare the expression of nitrate-responsive genes *NRT1.1* and *NRT2.1* in Col-0 and *hbi-q* in response to nitrate. When

seedlings were treated with nitrate for 3 h, like in the RNA-Seq experiments, we found that nitrate had similar inducing effects on the expression of *NRT1.1* and *NRT2.1* in wild-type plants and *hbi-q* mutants. However, when nitrate treatment was for 30 min, the nitrate-increased expression of *NRT1.1* and *NRT2.1* was significantly reduced in *hbi-q* mutant, suggesting that HBIs might play an important role in the early induction of *NRT1.1* and *NRT2.1* by nitrate (Figure 3, D and E). We validated these results using another internal control, *ACT2* (Supplemental Figure S6A). ChIP–qPCR analysis revealed that HBI1 directly binds to the promoters of *NRT1.1* and *NRT2.1* (Figure 3, F and G). Furthermore, protoplast transient gene-expression assays showed that HBI1 significantly induced the expression of *NRT1.1* and *NRT2.1* (Figure 3, H and I). These results indicated that HBIs play important roles in the nitrate regulation of downstream gene expression.

HBIs contribute to the nitrate-triggered ROS scavenging

A recent study reported that HBI1 controls the tradeoff between plant growth and immunity through the transcriptional regulation of ROS homeostasis (Neuser et al., 2019). The significant enrichment of ROS-related genes among HBI-affected nitrate-regulated genes suggested that ROS might play an important function in the HBI-mediated nitrate response (Supplemental Figure S6B). Peroxidases play critical roles in the ROS homeostasis of plants. Our transcriptomic analysis showed the expression of 14 peroxidases was regulated by nitrate treatment, of which 8 were upregulated and 6 were downregulated by nitrate. Mutation of *HBIs* significantly reduced the promoting effects of nitrate on the most of upregulated peroxidases, but only weak effects on the nitrate-repressed peroxidases (Supplemental Figure S6C). RT-qPCR analysis further confirmed that nitrate significantly induced the expression of peroxidase genes including *PRX5*, *PRX27*, *PRX28*, *PRX52*, and *PRX62*, and such promoting effects of nitrate were impaired in *hbi-q* mutants (Supplemental Figure S6D).

To determine whether nitrate regulates ROS levels in plants, we measured ROS content in wild-type plants and *hbi-q* mutants with or without nitrate treatment using the fluorescent dye 2′, 7′-dichlorofluorescin diacetate (H_2DCFDA) and nitroblue tetrazolium (NBT; Bielski et al., 1980; Yao and Greenberg, 2006). The nitrate treatment significantly reduced the ROS content in wild-type seedlings. Loss of functions of *HBIs* resulted in the high accumulation of ROS in the absence of nitrate and failure to effectively scavenge ROS after nitrate treatment (Figure 4, A to D; Supplemental Figure S7, A and B). These results indicate that nitrate induces scavenging of ROS through HBI-mediated increases in the expression levels of a set of antioxidant genes.

Catalase plays a critical role in HBI1-mediated plant growth

Catalase is a key H_2O_2 scavenging enzyme in plants (Su et al., 2018). Our RNA-Seq and RT-qPCR results revealed that nitrate induced the expression of *CAT2* through HBIs (Figure 5A; Supplemental Data Set S1). We selected CAT2 to determine whether the promoting effects of HBIs on plant growth are dependent on ROS scavenging. We observed that the overexpression of *HBI1* induced *CAT2* expression, and mutation in *HBIs* led to a decreased transcript of *CAT2*

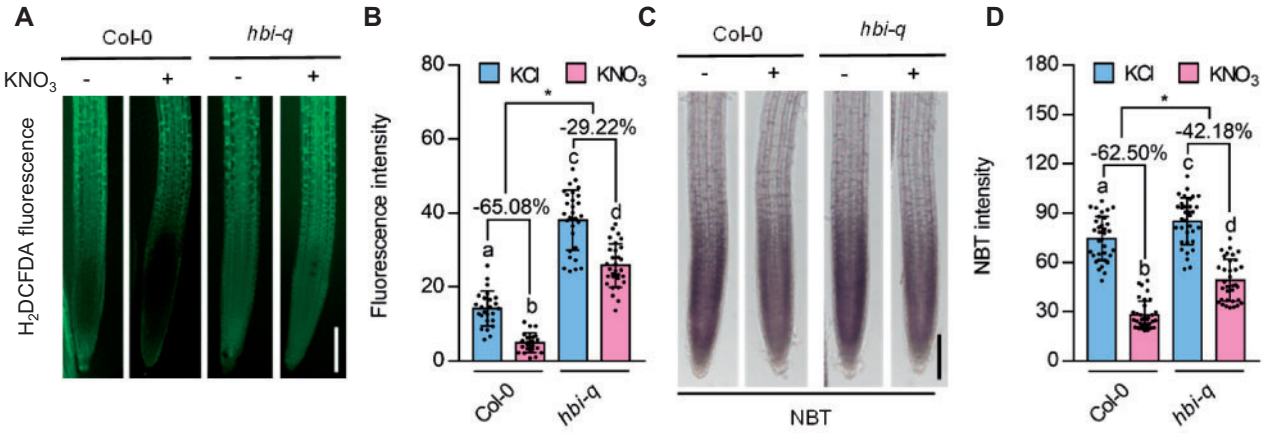

Figure 4 HBIs contribute to the nitrate-triggered ROS scavenging. A, H_2DCFDA staining for H_2O_2 in the primary root tips of the wild-type and *hbi-q* treated with KCl or KNO_3. Bar = 100 μm. Wild-type plants and *hbi-q* mutants growing on medium with 10-mM KNO_3 for 5 days were transferred to nitrogen-free medium for 2 days and then treated with 10-mM KCl or KNO_3 for 1 h. B, Quantification of H_2DCFDA fluorescence intensities in the images of (A). Error bars, SD (n = 22–29 images). C, NBT staining showed that nitrate treatment significantly reduced the contents of ROS in the primary roots of wild-type plants (Col-0), but had weak effects in those of *hbi-q*. Bar = 100 μm. Wild-type plants and *hbi-q* mutants growing on medium with 10-mM KNO_3 for 5 days were transferred to nitrogen-free medium for 2 days then treated with 10-mM KCl or KNO_3 for 1 h. D, Quantification of NBT intensities in the images of (C). Error bars, SD (n = 34 images). For (B) and (D), different letters above bars indicate statistically significant difference between samples (two-way ANOVA analysis followed by Tukey's test, $P < 0.05$). Asterisks between bars indicate statistically significant different effects of nitrate on the scavenging ROS in Col-0 and *hbi-q* (Student's t test, *$P < 0.05$).

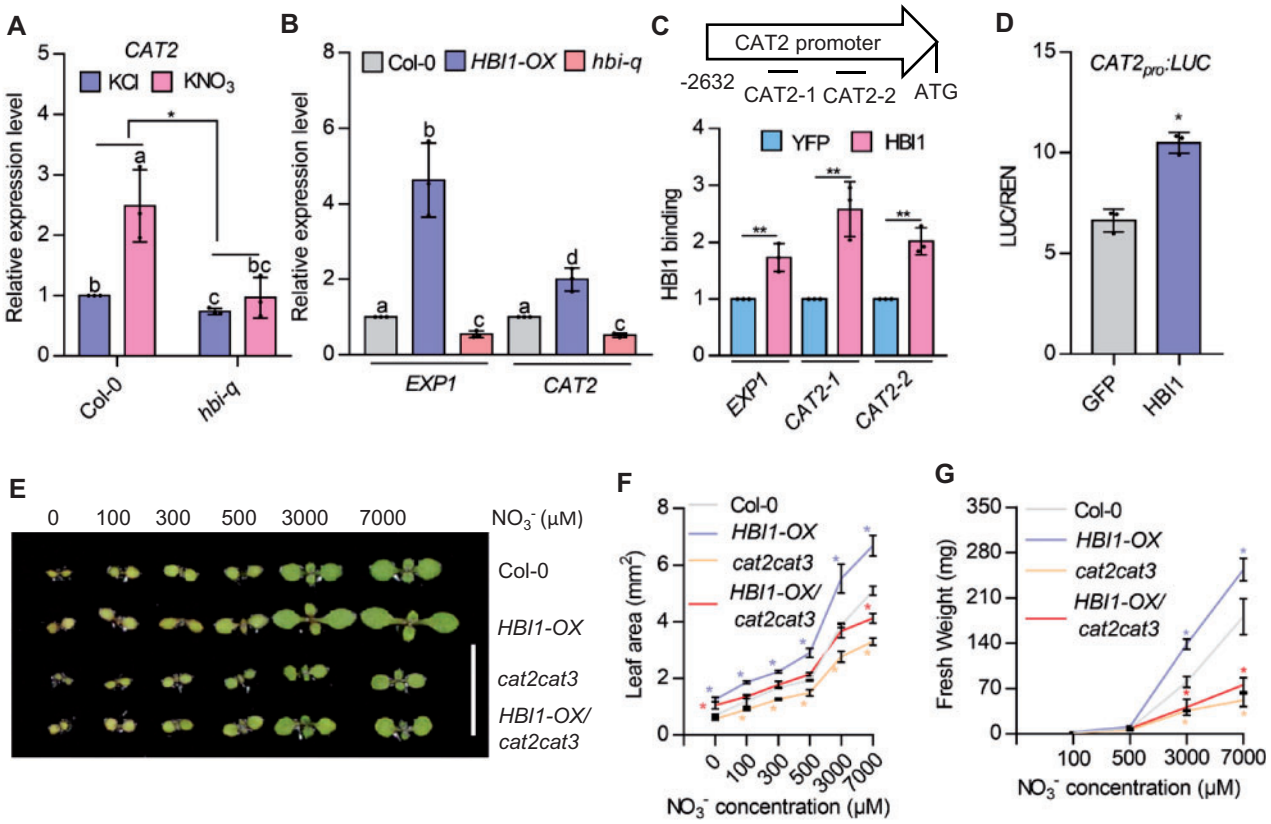

Figure 5 Catalase plays critical roles in HBI-promoted nitrate responses. A, HBIs are required for nitrate-induced the expression of *CAT2*. Seedlings of Col-0 and *hbi-q* grown on medium with 7-mM KNO_3 for 5 days were transferred to nitrogen-free medium for 2 days, and then treated with 10-mM KNO_3 for 3 h. The transcript levels of *CAT2* were quantified by real-time PCR. *PP2A* was used as an internal control. Error bars are SD of three biological replicates. Different letters above bars indicate statistically significant difference between samples (two-way ANOVA analysis followed by Tukey's test, $P < 0.05$). Asterisks between bars indicate statistically significant different effects of nitrate on the *CAT2* expression in the wild-type and *hbi-q* mutant (Student's *t* test, $^*P < 0.05$). B, RT-qPCR analysis of the expression of *CAT2* and *EXP1* in the wild-type, *HBI1-Ox*, and *hbi-q* that were grown on half-strength MS medium under 16-h light/8-h dark photoperiod for 7 days. *PP2A* was used as an internal control and *EXP1* was used as a positive control. Error bars indicate SD of three independent experiments. Different letters above bars indicate statistically significant differences between samples (one-way ANOVA analysis followed by Tukey's test, $P < 0.05$). C, HBI1 directly binds to the promoter of *CAT2*. The $35S_{pro}$:*HBI1-YFP* and $35S_{pro}$:*YFP* transgenic plants growing in half-strength MS liquid medium for 12 days were used to perform the ChIP analysis. Illustration of different regions in the promoter of *CAT2*. The levels of HBI1 binding were calculated as the ratio between $35S_{pro}$:*HBI1-YFP* and $35S_{pro}$:*YFP* control, and then normalized to that of the control gene *PP2A*. *EXP1* was used as a positive control. Error bars indicate SD of three independent experiments. Asterisks between bars indicate statistically significant differences between samples (Student's *t* test, $^*P < 0.05$). D, Transient assays showed HBI1 promotes the expression of *CAT2*. The *CAT2* promoter fused to the luciferase reporter gene was co-transfected with $35S_{pro}$:*GFP* or $35S_{pro}$:*HBI1-GFP* into mesophyll protoplasts of wild-type plants. The luciferase activities were normalized by Renilla luciferase as an internal control. Error bars indicate SD of three independent experiments. Asterisks between bars indicate statistically significant differences between samples (Student's *t* test, $^*P < 0.05$). E, F, Mutations of *CAT2* and *CAT3* suppressed the HBI1-promoted shoot growth. Seedlings of Col-0, *cat2cat3*, *HBI1-Ox*, and *HBI1-Ox/cat2cat3* were grown on medium with different concentrations of nitrate for 7 days. Scale bar represents 10 mm. Error bars indicate SD ($n = 24–36$). Asterisks indicate statistically significant differences between Col-0, *cat2 cat3*, *HBI1-Ox*, and *HBI1-Ox/cat2 cat3* (Student's *t* test, $^*P < 0.05$). G, Quantification of the fresh weight of the wild-type, Col-0, *cat2 cat3*, *HBI1-Ox*, and *HBI1-Ox/cat2 cat3* that were grown on the medium with different concentrations of nitrate under 16h light/8h dark for 4 weeks. Error bars indicate SD ($n = 15–26$). Asterisks indicate statistically significant differences between, *cat2 cat3*, *HBI1-Ox*, and *HBI1-Ox/cat2 cat3* (Student's *t* test, $^*P < 0.05$).

(Figure 5B). ChIP–qPCR analysis showed that HBI1 directly binds to the promoter of *CAT2* (Figure 5C). The analysis of the protoplast transient assays showed that HBI1 promoted the expression of *CAT2* (Figure 5D). These results indicated HBI1 directly promoted *CAT2* expression.

Next, we generated the *HBI1-Ox/cat2 cat3* plants by crossing *HBI1-Ox* transgenic plants with *cat2 cat3* mutants. The analysis of ROS content showed that nitrate treatment significantly reduced the ROS levels in the wild-type and *HBI1-Ox* plants, but had weaker effects in the *cat2 cat3* and *HBI1-Ox/cat2 cat3* (Supplemental Figure S8, A to D). In the wild-type background, overexpression of *HBI1* led to larger cotyledons and higher fresh weight compared to wild-type plants. However, mutation in *CAT2* and *CAT3* significantly reduced the promoting effects of HBI1 on plant growth (Figure 5, E to G; Supplemental Figure S9, A to E). These

results indicated that HBI1 might promote plant growth by promoting ROS scavenging through catalase.

H_2O_2 treatment inhibits the nitrate-mediated plant growth

To investigate whether ROS are involved in nitrate-mediated plant growth and development, we analyzed the growth phenotypes of wild-type plants and *cat2 cat3* mutants that were grown on medium with different nitrogen sources. In the presence of KCl, NH_4^+, or Gln, *cat2 cat3* and wild-type plants showed a similar growth phenotype. However, when grown on the medium with KNO_3, nitrate supply significantly stimulated shoot growth of wild-type plants, but had weaker effects on the growth of *cat2 cat3*, suggesting CAT2 and CAT3 are required for nitrate-promoted shoot growth (Supplemental Figure S9, D and E). To further examine the effects of ROS on nitrate-stimulated plant growth and development, we analyzed the growth phenotypes of wild-type plants and *cat2 cat3* mutants in the presence of different concentrations of nitrate and/or H_2O_2. Nitrate treatment promoted cotyledon expansion, stimulated shoot growth, and increased primary root length, total lateral root length and lateral root number in wild-type plants. However, mutations of *CAT2* and *CAT3* or co-treatment with H_2O_2 strongly counteracted the effects of nitrate on plant growth and development (Figure 6, A to G). Additionally, we analyzed the effects of different concentrations of H_2O_2 on plant growth at the same nitrate concentration and found that the length of primary roots and the number of lateral roots were significantly reduced with increasing H_2O_2 concentration, indicating that H_2O_2 inhibited root growth and development in a dose-dependent manner (Supplemental Figure S10, A–D). These results suggested that nitrate-mediated removal of ROS contributes to nitrate-induced plant growth and development.

H_2O_2 treatment inhibits the regulation of gene expression by nitrate

To determine the effects of ROS on the nitrate-regulated gene expression, we performed RT-qPCR in the wild-type and *cat2 cat3* with or without nitrate treatment. RT-qPCR analysis showed that mutations of *CAT2* and *CAT3* significantly inhibited the nitrate-induced expression of *NRT1.1* and *NRT2.1* (Supplemental Figure S11, A and B). NRP-YFP is a nitrate-responsive marker line (Wang et al., 2009). Nitrate treatment significantly increased the fluorescence intensity of NRP-YFP in the wild-type background, but such effects of nitrate were impaired in *cat2 cat3* mutants (Supplemental Figure S11, C and D). These results indicated that CAT-mediated scavenging of ROS plays an important role in the nitrate signaling pathway.

To further determine the roles of ROS in nitrate-regulated gene expression at the genomic level, we performed the RNA-Seq experiments with the wild-type Col-0 grown on MGRL medium (7-mM nitrate) for 7 days. After this period, nitrate starvation was imposed for 2 days, and then plants were treated with 10-mM KCl, 10-mM KNO_3 and/or 0.5-mM H_2O_2 for 3 h. There were 3,431 genes affected with more than two-fold changes by only nitrate treatment, 1,810 genes regulated by only H_2O_2 treatment, and 2,382 genes regulated by nitrate and H_2O_2 co-treatment (Figure 6H; Supplemental Data Sets S1, S5, and S6). The genes regulated by only nitrate or only H_2O_2 treatment did not display a clear regulation pattern, which may be due to the experimental conditions we used to carry out RNA-Seq (Supplemental Figure S12, A and B). Before the plants were treated with nitrate or H_2O_2, the plants were grown on nitrate-free medium for 2 days, which resulted in high accumulation of ROS in plants. However, among 3,431 genes regulated by nitrate under normal conditions, 1,811 genes (52.8%) were no longer responsive to nitrate when co-treated with H_2O_2; we termed these H_2O_2-counteracted nitrate-responsive genes, and the other 1,620 genes were termed H_2O_2-unaffected nitrate-responsive genes (Figure 6, H and I). GO analysis showed that terms related to nitrate-regulated genes, response to nitrogen compound, starvation, nutrient levels, oxidoreductase activity, anion transport, starch metabolism, and gibberellin metabolic processes were highly enriched in the H_2O_2-counteracted nitrate-regulated genes (Supplemental Figure S13). These results demonstrated that H_2O_2 plays a negative role in nitrate signal transduction.

To further determine whether NLP7 and HBIs are involved in the H_2O_2–counteracted gene expression in response to nitrate, we compared the NLP7- or HBI-affected nitrate-responsive genes with H_2O_2-counteracted nitrate-responsive genes. The results showed that most of H_2O_2-counteracted nitrate-responsive genes are not regulated by nitrate in *nlp7-1* mutants, and most NLP7-unaffected nitrate-responsive genes are also not affected by H_2O_2 treatment (Figure 6J), suggesting NLP7 plays critical roles in the H_2O_2 inhibition of nitrate-regulated downstream gene expression. Among the 764 HBI-affected nitrate-responsive genes, 672 genes (88%) were regulated by nitrate through the H_2O_2-counteracted pathway, whereas among H_2O_2-counteracted nitrate-responsive genes, HBI-dependent nitrate-responsive genes were not enriched (Figure 6K), indicating that HBIs are not the targets of H_2O_2 in inhibiting nitrate-regulated gene expression. These transcriptomic analyses, together with genetic data showing the catalase is required for the functions of HBIs, indicated that HBIs regulate plant growth and gene expression in response to nitrate by modulating ROS homeostasis in plants.

H_2O_2 inhibits the nitrate-triggered nuclear localization of NLP7

Considering that >50% of nitrate-responsive genes are counteracted by H_2O_2 supply, we speculated that the key components of nitrate signaling pathways were the targets of H_2O_2. To determine which key components of nitrate signal transduction are regulated by H_2O_2, we compared the difference in nitrate-induced phosphorylation of NLP7

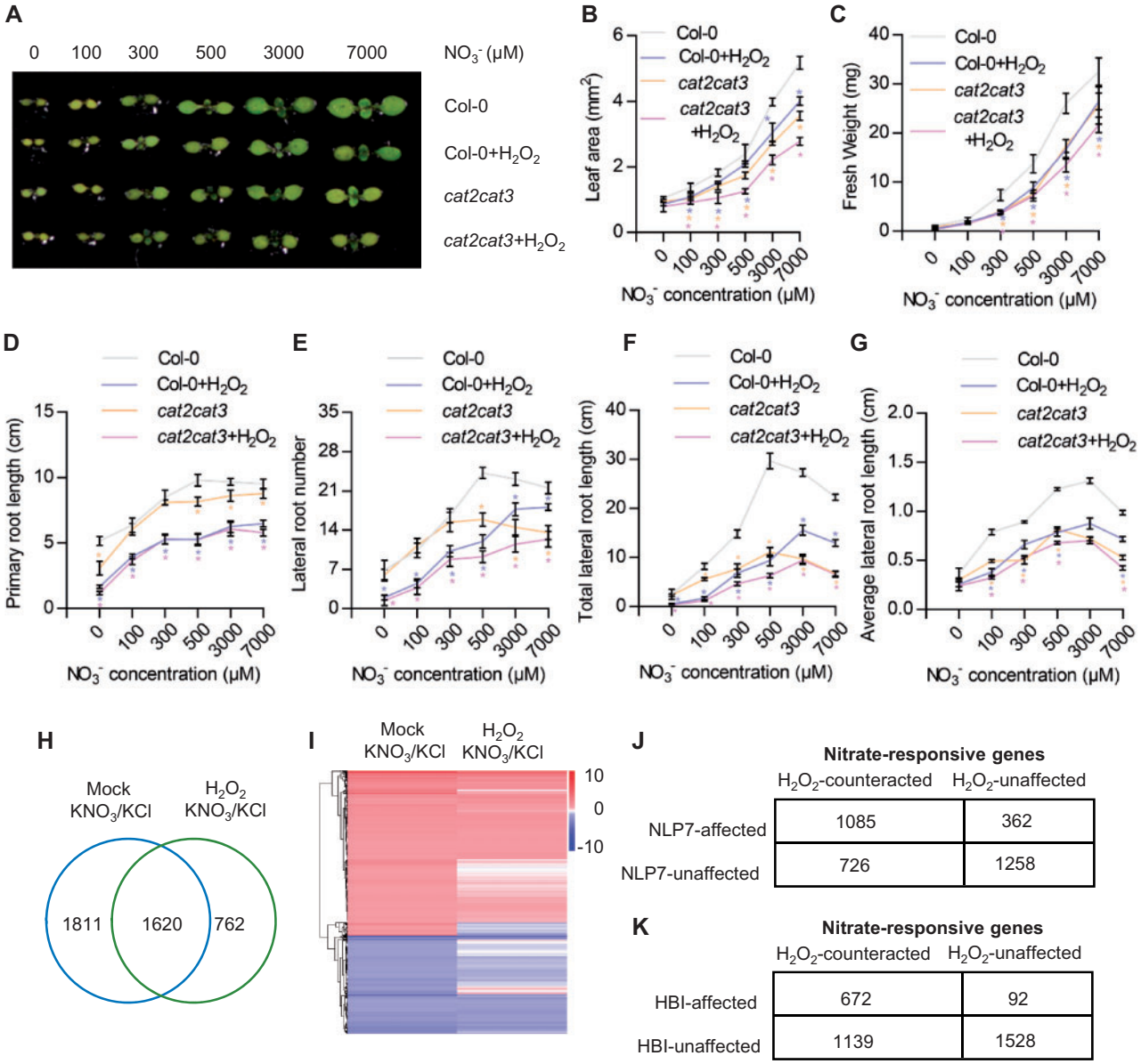

Figure 6 H_2O_2 negatively regulates the nitrate-mediated plant growth and gene expression. A, Seedlings of wild-type plants and *cat2 cat3* mutants grown on medium containing different concentrations of nitrate with or without 0.5-mM H_2O_2 for 7 days. Scale bar represents 10 mm. B, Measurement of the cotyledon area of plants in (A). Error bars indicate SD (n = 16–28). Asterisks indicate statistically significant differences between Col-0 and *cat2 cat3* at individual concentration (Student's t test, $^*P < 0.05$). C, Measurement of the fresh weight of the wild-type and *cat2 cat3* grown on medium containing different concentrations of nitrate with or without 0.5-mM H_2O_2 for 15 days. Error bars indicate SD (n = 21–30). Asterisks indicate statistically significant differences between Col-0 and *cat2 cat3* at individual concentration (Student's t test, $^*P < 0.05$). D–G, H_2O_2 inhibited the nitrate-regulated root development. Wild-type and *cat2cat3* seedlings were grown on medium with or without 0.5-mM H_2O_2 and different concentrations KNO_3 for 12 days. Primary root length (D), lateral root number (E), total lateral root length (F), and average lateral root length (G) were quantified. Error bars indicate SD (n = 30). Asterisks indicate statistically significant differences between Col-0 and *cat2 cat3* at individual concentration (Student's t test, $^*P < 0.05$). H, Venn diagram showing the overlap between sets of genes significantly regulated by nitrate in the wild-type with or without H_2O_2 treatment. I, Hierarchical cluster analysis of the expression data of 3,431 genes regulated by nitrate in wild-type plants with or without H_2O_2 treatment. The numerical values for the blue-to-red gradient bar represent $\log_2$ of the ratio. J, K, Comparison of the HBI- or NLP7-affected nitrate-responsive genes with H_2O_2-counteracted nitrate-responsive genes.

proteins with or without H_2O_2 treatment. We reasoned that if H_2O_2 could alter the phosphorylation levels of NLP7, H_2O_2 may target upstream of NLP7, possibly the transceptor NRT1.1 or kinase CPKs; conversely, if H_2O_2 had no significant effect on the phosphorylation of NLP7, H_2O_2 may act on NLP7 itself or downstream of NLP7. Immunoblot analysis showed that nitrate treatment caused the phosphorylation of NLP7, but co-treatment with H_2O_2 had no obvious effect on the levels of phosphorylated NLP7 (Figure 7A; Supplemental Figure S14), thus indicating that H_2O_2

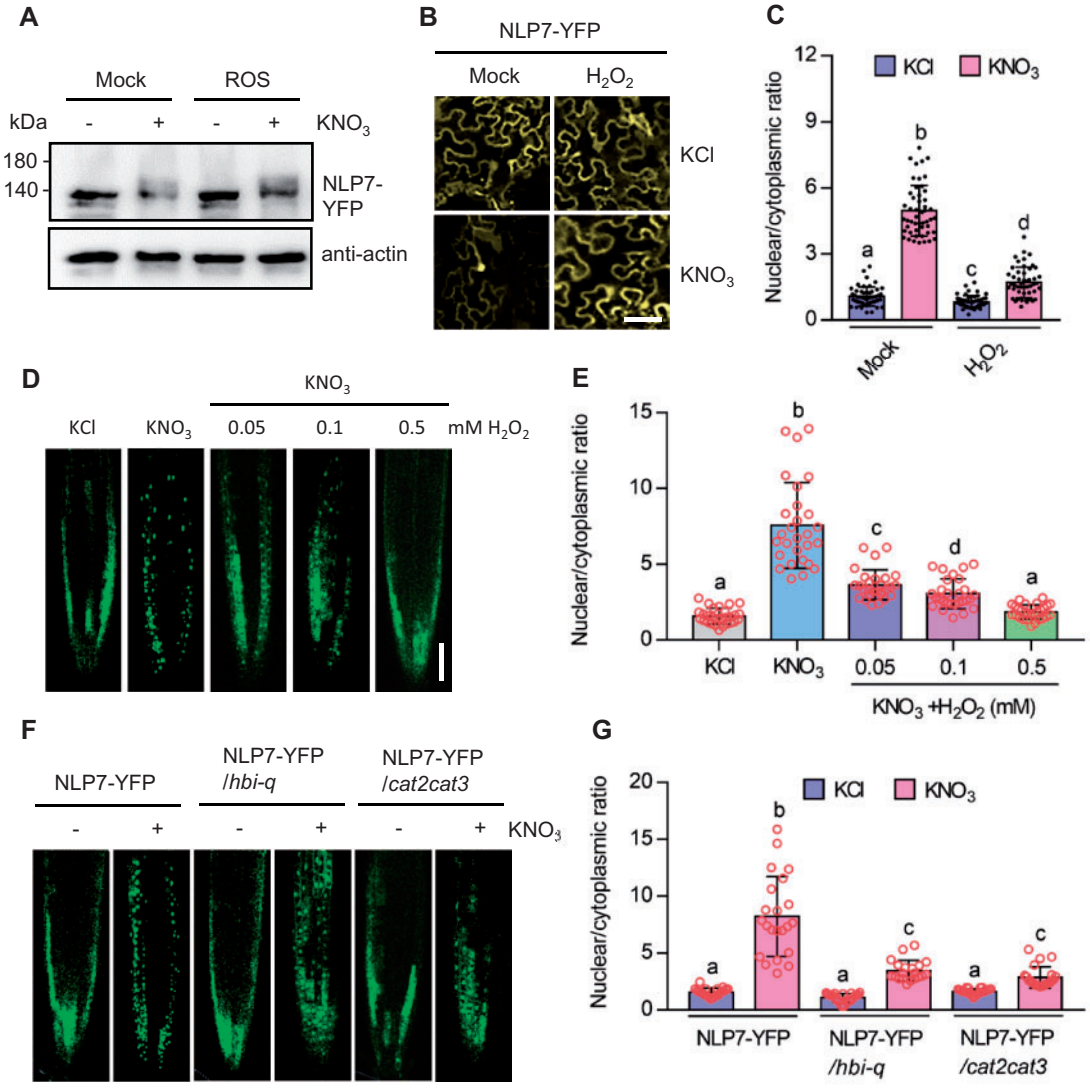

Figure 7 H_2O_2 attenuates the nitrate-induced nuclear localization of NLP7-YFP. A, H_2O_2 treatment had no significant effects on nitrate-induced phosphorylation of NLP7. The immunoblots were probed using anti-YFP and anti-actin antibodies. Actin bands showed protein loading. Transgenic plant $35S_{pro}$:*NLP7-YFP* growing on medium with 10-mM KNO_3 for 5 days were transferred to nitrogen-free medium for 2 days, and then treated with 10-mM KCl, KNO_3, and/or 0.5-mM H_2O_2 for 0.5 h. B, C, H_2O_2 inhibited the nitrate-induced nuclear localization NLP7-YFP in the epidermal cells of *N. Benthamiana*. Plants that were scooped out from soil and grown on the nitrate-free medium for 2 days were transformed with *Agrobacterium* containing $35S_{pro}$:*NLP7-YFP* construct. After 36 h, these plants were treated with 10-mM KCl, 10-mM KNO_3, and/or 0.5-mM H_2O_2 for 1 h. Scale bar: 10 μm. Different letters above the bars indicate statistically significant differences between the samples (two-way ANOVA analysis followed by Tukey's test, $P < 0.05$). D, E, H_2O_2 antagonizes nitrate in the regulation of the nuclear localization of NLP7-YFP in plants. Seedlings of $35S_{pro}$:*NLP7-YFP* transgenic plants were grown on the medium with or without 10-mM KCl, 10-mM KNO_3, and/or different concentrations of H_2O_2 for 7 days. Scale bar, 50 μm. Different letters above the bars indicate statistically significant differences between the samples (one-way ANOVA analysis followed by Tukey's test, $P < 0.05$). F, G, Nitrate-induced nuclear localization of NLP7-YFP was impaired in *hbi-q* and *cat2 cat3* mutants. Seedlings of $35S_{pro}$:*NLP7-YFP*, $35S_{pro}$:*NLP7-YFP/hbi-q*, and $35S_{pro}$:*NLP7-YFP/cat2 cat3* were grown on medium containing 10-mM KCl or 10-mM KNO_3 for 7 days. Scale bar: 50 μm. Fluorescent signals were visualized by using the LSM-700 laser scanning confocal microscope (Zeiss) and the signal intensities of YFP were determined by ImageJ software. Error bars, SD (n = 28 images). Different letters above the bars indicate statistically significant differences between the samples (two-way ANOVA analysis followed by Tukey's test, $P < 0.05$).

probably regulates nitrate signal transduction through the transcription factor NLP7 or downstream of NLP7.

To understand how H_2O_2 modulates the function of NLP7 in plants, we examined whether H_2O_2 affects the subcellular localization of NLP7 by analyzing NLP7-YFP proteins in the epidermal cells of *Nicotiana benthamiana* leaves. NLP7 was fused to YFP and then transiently expressed in the leaves of *N. benthamiana*, which were first grown in the soil to the 3- to 4-leaf stage, then washed with water to clean off soil particles, and transferred to a nitrogen-deficient hydroponic solution for about 48 h. Under nitrogen starvation, a few fluorescent signals of NLP7-YFP were

found in the nucleus, and most fluorescent signals were found outside the nucleus. Nitrate treatment induced the nuclear localization of NLP7-YFP and the ratio of nuclear to cytoplasmic NLP7-YFP was significantly increased. However, co-treatment with nitrate and H_2O_2 significantly attenuated the nitrate-induced transport of NLP7-YFP from the cytoplasm to the nucleus (Figure 7, B and C). These findings were validated in the primary roots of the *35S$_{pro}$:NLP7-YFP* and *NLP7$_{pro}$:NLP7-YFP* transgenic plants. Nitrate supply significantly induced the nuclear localization of NLP7-YFP, while in the presence of 0.05-mM H_2O_2, such effects of nitrate on the subcellular location of NLP7-YFP were slightly reduced. As the concentration of H_2O_2 increased, a growing amount of NLP7-YFP was localized in the cytoplasm, indicating H_2O_2 inhibits the nitrate-induced nuclear localization of NLP7 in a dose-dependent manner (Figure 7, D and E; Supplemental Figure S15, A and B). Leptomycin B (LMB) is a streptomycin metabolite that inhibits the export of nuclear proteins (Haasen et al., 1999). LMB treatment abolished the inhibiting effects of H_2O_2 on the nuclear localization of NLP7 (Supplemental Figure S16, A and B). To further determine the specific effects of H_2O_2 on the subcellular location of HBI1, we analyzed the subcellular localization of HBI1-YFP in the presence of nitrate and/or H_2O_2. The results showed that nitrate and H_2O_2 had no significant effects on the subcellular localization of HBI1-YFP (Supplemental Figure S17, A and B). These results indicated that H_2O_2 treatment reduces the nitrate-triggered nuclear localization of NLP7.

To corroborate these pharmacologic data, we analyzed the effects of H_2O_2 on the subcellular location of NLP7 in the *cat2 cat3* and *hbi-q* mutants, which accumulate high levels of H_2O_2. The results showed that nitrate treatment significantly induces the nuclear localization of NLP7-YFP, but such effects of nitrate were reduced in *hbi-q* and *cat2 cat3* mutants (Figure 7, F and G). Furthermore, we found overexpression of *HBI1* promoted the nuclear localization of NLP7 in response to nitrate (Supplemental Figure S18, A and B). NLP6, the homolog of NLP7, also showed nitrate-induced nuclear localization, whereas in the presence of H_2O_2, NLP6 was retained in the cytoplasm (Supplemental Figure S19, A–D). These results indicated that H_2O_2 inhibited the nitrate-induced nuclear localization of NLP6 and NLP7.

Discussion

Nitrate is the main form of nitrogen that affects plant growth and crop yield and also an important molecular signal for plant adaptation to changing soil conditions (Xu et al., 2012; O'Brien et al., 2016; Wang et al., 2018b). Nitrate binding to the dual-affinity transceptor NRT1.1 triggers the accumulation of calcium in plants, which in turn activates three CPKs to phosphorylate and promote the nuclear location of NLP7 (Liu et al., 20017). In this study, we further showed that the bHLH transcription factors HBI1 and BEE2 are targets of NLP7. Nitrate-activated NLP7 directly induces the expression of *HBI1* and *BEE2*, which then promotes ROS scavenging in plants by directly regulating the expression of *CAT2*. Mutation in *HBI* genes resulted in ROS accumulation, and about 22% of nitrate-responsive genes were no longer regulated by nitrate. Exogenous H_2O_2 treatment repressed the nitrate-stimulated plant growth and downstream gene expression by inhibiting the nuclear localization of NLP7. Nitrate treatment reduced the accumulation of H_2O_2, and H_2O_2 inhibits nitrate signaling, thereby forming a feedback regulatory loop to regulate plant growth and development (Figure 8).

HBI1 has been reported to integrate diverse environmental, phytohormone, and plant pathogen signals to regulate plant growth and immunity (Bai et al., 2012; Fan et al., 2014). Here, we further demonstrate through several lines of evidence that HBI1 and its homologs participate in nitrate signaling. First, HBI1 and BEE2 are the early nitrate-responsive genes. Nitrate treatment induces *HBI1* and *BEE2* expression in as little as 15 min. Second, HBIs play critical roles in the nitrate-regulated gene expression. Transcriptomic analysis showed that ~22% of the genes were no longer responsive to nitrate in *hbi-q*. Nitrate supply significantly induces the expression of *NRT1.1* and *NRT2.1*, whereas such effects of nitrate were reduced in *hbi-q* mutants. HBI1 could directly bind to the promoters of *NRT1.1* and *NRT2.1* to induce their expression. Third, HBIs are involved in nitrate-stimulated plant growth and development. The plants lacking HBI1 and its three homologs displayed similar growth phenotypes to that of wild-type plants when grown on the medium with KCl or NH_4^+, but exhibited deficiency in nitrate promotion of plant growth

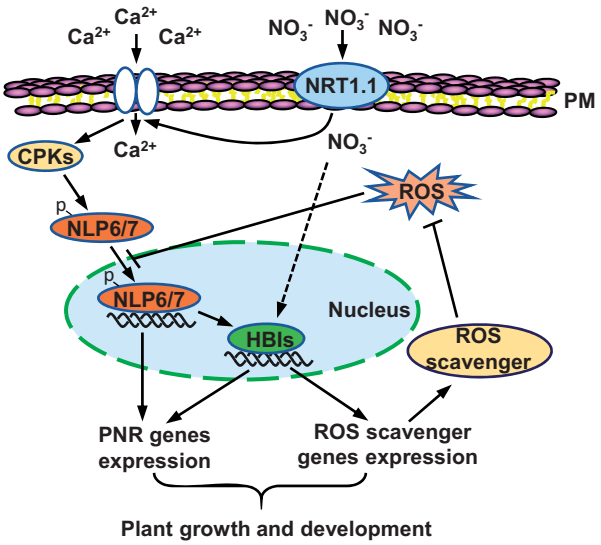

Figure 8 A model for the contribution of HBIs in nitrate-mediated gene expression and plant growth. Perception of nitrate signals by the transceptor NRT1.1 triggers the phosphorylation and nuclear localization of NLP6 and NLP7 to induce the expression of *HBIs*. HBIs not only regulate some of nitrate-responsive gene expression, but also increase the expression levels of a set of antioxidant genes to reduce the accumulation of H_2O_2, which inhibits the nitrate-induced nuclear localization of NLP6 and NLP7, thereby forming a feedback regulatory loop to enhance the nitrate signaling in plants. P, phosphorylation; PM, plasma membrane.

and development, suggesting that HBIs play important roles in nitrate-mediated plant growth. Overexpression of *HBI1* led to the increased shoot growth and root development phenotype in all growth conditions, which may be due to dual functions of HBI1 in plant growth. On the one side, HBI1 could induce the expression of ROS scavenging genes to reduce the ROS content in the plant and then activate NLP7 to regulate downstream gene expression. On the other side, HBI1 could directly bind to the promoters of growth-related genes to induce the expression of these genes and promote plant growth. Furthermore, the *chl1-5* partially suppressed the increased growth phenotypes of *HBI1-Ox* plants. Together, these results revealed that HBIs positively regulate nitrate signaling to control plant growth and development.

ROS are involved in numbers of signaling pathways and their homeostasis affects many developmental processes and responses to diverse biotic and abiotic stresses (Mittler, 2017; Waszczak et al., 2018). Previous studies reported that nitrate starvation induces the accumulation of ROS (Safi et al., 2018). Here, we showed that nitrate supply reduces the ROS levels by inducing the expression of antioxidant genes such as peroxidases, glutaredoxin, and catalase. HBIs play an important role in the transcriptional induction of this detoxification program. HBI1 directly binds to the promoter of *CAT2* to induce its expression and reduce the ROS content in plants. However, nitrate had weak but still significant effects on the induction of antioxidant gene expression in *hbi-q* mutants, suggesting that other regulatory factors are involved in the nitrate-mediated expression of these antioxidant genes. A recent study showed that the chromatin factor HIGH NITROGEN INSENSITIVE9 (HNI9) and transcription factor ELONGATED HYPOCOTYL5 (HY5) regulate the ROS homeostasis of plants in response to high nitrate provision through the induction of a subset of antioxidant genes (Bellegarde et al., 2019). Mutations of *HNI9* or *HY5* lead to the highly accumulated ROS under high nitrate provision. Transcriptomic analysis showed that HNI9 and HY5 induced the expression of numbers of genes involved in ROS scavenging in response to high nitrate provision. HNI9 has been reported to interact with BES1, a master transcription factor of brassinosteroid (BR) signaling, to promote downstream gene expression (Li et al., 2010). BR and BES1 increase the activity of HBI1 by activating an HLH/bHLH tripartite growth regulatory cascade (Bai et al., 2012). Thus, HBIs, HNI9, and HY5 form a transcriptional regulator network that modulates the expression of ROS-related genes to fine-tune the ROS homeostasis in response to fluctuating external nitrate supply.

H_2O_2 is an important redox signaling molecule that is involved in plant developmental processes and stress responses, due to its remarkable universality within cells and the reversible oxidation of target proteins (García-Santamarina et al., 2014; Waszczak et al., 2018). In the present study, we demonstrated that H_2O_2 negatively regulates nitrate signal transduction through modulating the subcellular location of NLP7. Under nitrate deprivation, the expression of *HBIs* is not induced, which leads to the low expression of antioxidant genes and H_2O_2 accumulation, thereby inhibiting plant growth. Constitutive expression of *HBI1* reduced the H_2O_2 levels and partially rescued the growth defect in the low-nitrate conditions. The *hbi-q* and *cat2 cat3* mutants, which accumulate high levels of H_2O_2, had impaired nitrate-regulated downstream gene expression. Transcriptomic analysis showed that more than half of the nitrate-regulated genes were no longer responsive to nitrate in the presence of H_2O_2, and most H_2O_2-counteracted nitrate-responsive genes were regulated by nitrate through the NLP7-dependent pathway, indicating that H_2O_2 inhibits the regulatory effects of nitrate on downstream gene expression through modulating the activity of NLP7. Furthermore, nitrate treatment induced the nuclear localization of NLP7, whereas such promoting effects of nitrate were significantly reduced by co-treatment with H_2O_2 or mutation of *HBI* or *CAT* genes. The overexpression of *HBI1* slightly increased the nuclear localization of NLP7 in the absence of nitrate, suggesting that other signals might regulate the nuclear location of NLP7, and HBI1 may have a function in this process. These results demonstrated that H_2O_2 contributes to nitrate signal transduction partially through regulating the nucleocytoplasmic shuttling of NLP7.

As a molecular signal, H_2O_2 generally regulates the activity of target proteins through cysteine oxidative modification of the target proteins. For example, H_2O_2 has been reported to induce the oxidation of BZR1, a master regulator in the signaling pathway for the plant hormone brassinosteroid. Oxidative modification enhanced the transcription activity of BZR1 through increasing the binding affinity of BZR1 to its partners PIF4 and ARF6 (Tian et al., 2018). Here, we showed that H_2O_2 regulates the subcellular location of NLP7 to negatively modulate the nitrate signal transduction, but its molecular mechanism remains unclear. One possibility is that H_2O_2 directly induces the oxidative modification of NLP7. NLP7 contains 25 cysteine residues, which may be the putative target sites of oxidation. Two of them, Cys273 and Cys296, are located in the NLP7 GAF-like domain that is the nitrate-responsive domain; two of them, Cys615 and Cys623, are located in the RWP-PK domain that is the DNA binding domain; two of them, Cys919 and Cys926, are located in the PB1 domain that is protein–protein interaction domain. Site-directed mutagenesis of these cysteines to analyze their effects on the subcellular location of NLP7 will help to reveal whether H_2O_2 modulates the subcellular location of NLP7 through oxidative modification of these cysteines. Another possibility is that H_2O_2 induces the oxidative modification of the partners of NLP7. *OsNLP3* is the closest homolog of *NLP7* in rice. Nitrate treatment significantly induced the nuclear location of OsNLP3, and mutation in *OsNLP3* caused a severe defect in nitrate-induced gene expression, indicating OsNLP3 plays an important role in the rice nitrate signaling pathway (Hu et al., 2019). A recent study showed that OsNLP3 physically interacts with OsSPX4 and OsPHR2, which are the key transcription factors of the phosphate signaling pathway. These interactions increase the cytoplasmic retention of

OsNLP3 and OsPHR2, and repress the downstream phosphate and nitrate responses (Hu et al., 2019). H_2O_2 might induce the oxidation of OsSPX4 to enhance the interaction between OsSPX4 and OsNLP3, thereby increasing the cytoplasmic retention of OsNLP3.

ROS and calcium (Ca^{2+}), acting as ubiquitous secondary messengers in the cell, exhibit crosstalk to regulate many cellular processes. Both ROS and Ca^{2+} are involved in nitrate signaling. Ca^{2+} positively regulates nitrate signal transduction in plants, whereas ROS negatively regulates it. Using the ultrasensitive Ca^{2+} biosensors GCaMP6s and a nuclear mCherry, time-lapse recordings in single cells revealed that nitrate specifically stimulates a unique and dynamic Ca^{2+} signature in the nucleus and cytosol. Ca^{2+}-activated protein kinases CPK10, CPK30, and CPK32 phosphorylate NLP7 to promote its nuclear localization and regulate the nitrate-responsive gene expression (Liu et al., 2017). Here, we showed that nitrate supply reduces the ROS accumulation by promoting the expression of ROS-scavenging genes. ROS treatment inhibits the nitrate-triggered nuclear localization of NLP7 to repress the nitrate signaling. ROS and Ca^{2+} antagonize to regulate nitrate signal transduction by modulating the nuclear localization of NLP7. Ca^{2+} has been reported to regulate the ROS level by binding directly to the EF-hand motif in the N-terminus of RBOH protein (Ogasawara et al., 2008), and/or by regulating the activities of CPK5 and CIPK26, which induce the phosphorylation of RBOH proteins (Kobayashi et al., 2007; Drerup et al., 2013). ROS regulate the change of Ca^{2+} by directly modulating the Ca^{2+} channel or pump, such as ROS-activating Ca^{2+}-permeable channels in root cells and Ca^{2+}-influx channels in stomates. However, how the production of ROS and Ca^{2+} are coordinated in the process of nitrate signaling remains to be further studied.

When plants are grown under the biotic or abiotic stress conditions, the nitrate content significantly decreases in both the leaves and roots (Song et al., 2019), compared to that under normal conditions, but the molecular mechanism remains unclear. Given that ROS generation is induced by diverse biotic and abiotic stresses, it would be expected that the biotic and abiotic stresses promote the cytoplasmic retention of NLP7 by inducing the accumulation of ROS in plants, thereby inhibiting the nitrate signal transduction and affecting the nitrate utilization efficiency of plants. Taken together, redox regulation of NLP7 sets a molecular framework for H_2O_2 crosstalk between nitrate signaling and plant stress responses. This mechanism of crosstalk is likely to provide insight into the molecular mechanisms involved in stress inhibition of nitrate utilization efficiency. Further, adequate regulation of the activity of key components in the nitrogen signaling pathway should improve plant tolerance to different stress conditions.

Materials and methods

Plant materials and growth conditions

Arabidopsis ecotype Columbia (Col-0) was used as the wild-type. Mutants *hbi1* (CS870840), *bee2* (Salk_205833) *bhlh031* (CS879790), and *bhlh079* (Salk_142716) were obtained from the Arabidopsis Biological Resource Centre (ABRC). Homozygous T-DNA lines were identified using HBI gene-specific primers and T-DNA left-border primers. The gene specific primers used are listed in Supplemental Data Set S7. The higher-order mutants were obtained by genetic crosses between *hbi1*, *bee2*, *bhlh031*, and *bhlh079*, and confirmed by PCR (Chu et al., 2020). The $35S_{pro}$:*HBI1-YFP* (*HBI1-Ox*), $35S_{pro}$:*NLP7-YFP* (*NLP7-Ox*), $NLP7_{pro}$:*NLP7-YFP*, *nlp7-1*, *nlp6-1 nlp7-1*, and *cat2 cat3* have been described previously (Huang et al., 1996; Bai et al., 2012; Li et al., 2015; Xu et al., 2016; Guan et al., 2017; Su et al., 2018; Chu et al., 2020). Seeds were either surface sterilized and plated on half-strength MS basal salt medium (Phyto-Technology Laboratories) or grown directly in soil. *Arabidopsis thaliana* plants were grown in a greenhouse or in a growth chamber under a 16-h/8-h light/dark cycle (white fluorescent lamp [intensity of 100–120 μmol m^{-2} s^{-1}]) at 22–24°C for general growth and seed harvesting. For short-term (1–3 weeks) hydroponic culture (for nitrate-induction assays and gene expression analyses), wild-type Col-0 seedlings and different mutants were cultivated in a growth chamber under a 16-h/8-h light/dark cycle at 22–24°C. In order to analyze the effect of different nitrate concentrations on plant growth, seeds were germinated and grown on MGRL medium consisting in 1.5-mM KH_2PO_4, 2-mM K_2HPO_4, 1.5-mM $MgSO_4$, 2-mM $Ca(NO_3)_2$, 3-mM KNO_3, 67-μM Na_2EDTA, 8.6-μM $FeSO_4$, 10.3-μM $MnSO_4$, 30-μM H_3BO_3, 1-μM $ZnSO_4$, 24-nM Na_2MoO_4, 130-nM $CoCl_2$, 1-μM $CuSO_4$, 0.05% MES, 1% sucrose, and 1% agar, among which $Ca(NO_3)_2$ and KNO_3 are replaced by $CaCl_2$ and KCl, depending on nitrate concentration. For root length measurement, seedlings were photocopied, and their primary roots and lateral roots were measured using Image J software (http://rsb.info.nih.gov/ij). Statistical analysis was performed with one-way or two-way ANOVA analysis followed by Tukey's test, $P < 0.05$, or Student's *t* test, $^*P < 0.05$ (Supplemental Data Set S8).

Plasmid constructs and transgenic plants

Full-length cDNA of *HBI1*, *NLP7* without stop codon were amplified by PCR and cloned into pENTR™/SD/D-TOPO™ vectors (Thermo Fisher), and then recombined with destination vector pGAL4BDGW (N-GAL4BD), pGAL4ADGW (N-GAL4AD), pX-nYFP ($35S_{pro}$:C-nYFP), pX-cYFP ($35S_{pro}$:C-cYFP), pDEST15 (N-GST), and pMAL2CGW (N-MBP). The ~2.1-kb promoters of *NRT1.1* and ~2-kb promoter of *CAT2* were amplified from Arabidopsis genomic DNA and cloned into the pENTR™/SD/D-TOPO™ vectors (Thermo Fisher), and then recombined with destination vector pGREEN-GW (*Promoter: LUC*). The ~1.2-kb promoter of *HBI1* was amplified and constructed into a vector to drive the expression of the luciferase gene. Then $HBI1_{pro}$:*LUC* transgenic plants were generated by *Agrobacterium* (GV3101)-mediated transformation by floral dip. Oligo primers used for cloning are listed in Supplemental Data Set S7.

Transient gene expression assays

Protoplast isolation and PEG transformation was carried out as described previously (Yoo et al., 2007; Wu et al., 2009).

Plasmid DNAs were extracted using the Qiagen Plasmid Maxi Kit according to manufacturer instructions. Aliquots of 5×10^4 isolated mesophyll protoplasts were transfected with a mixture of 20 μg of DNA and incubated overnight. Protoplasts were harvested by centrifugation and lysed in 100 μL of passive lysis buffer (Promega). Firefly and Renilla (as internal standard) luciferase activities were measured using a dual-luciferase reporter kit (Promega).

RNA isolation, RT-PCR, and RT-qPCR

Wild-type plants were grown on nitrate concentration gradient medium for 14 days; wild-type and *hbi-q* growing on medium with 7-mM KNO_3 for 7 days were transferred to nitrogen-free medium for 2 days and then treated with 10-mM KNO_3 at different times, or treated with 10-mM KNO_3, 0.5-mM H_2O_2 for 3 h, respectively. Whole plants were harvested and rapidly frozen in liquid nitrogen. Total RNA was extracted using the Trizaol RNA extraction kit (Transgene). The first-strand cDNAs were synthesized by RevertAid reverse transcriptase (Thermo) and used as RT-PCR templates. Q-PCR analyses using a SYBR green reagent (Roche) was carried on a CFX connect real-time PCR detection system (Bio-Rad) with gene-specific primers (see Supplemental Data Set S7).

ChIP-qPCR assay

ChIP assays were performed as described previously using $35S_{pro}$:*YFP*, $35S_{pro}$*NLP7-YFP*, and $35S_{pro}$:*HBI1-YFP* transgenic plants (Bai et al., 2012). Briefly, plants were grown in liquid half-strength MS medium containing 1% sucrose under a 16-h/8-h light/dark cycle for 12 days. The seedlings were cross-linked for 10 min in 1% formaldehyde and quenched by 0.25 M glycerine. Total chromatin was extracted and sonicated into fragments with sizes below 200 bp by Bioruptor (Diagenode), immunoprecipitation was performed using YFP-Trap bound to Protein A agarose. Immunoprecipitated protein and DNA were eluted with 1% SDS and 0.1 M $NaHCO_3$, and the crosslink was reversed by incubation at 95°C 1 h in the presence of 250-mM NaCl. DNA was extracted by a PCR purification kit (Fermentas) and analyzed by qPCR using the oligonucleotide primers listed in Supplemental Data Set S7. The enrichment was calculated as the ratio between $35S_{pro}$:*NLP7-YFP* and the $35S_{pro}$:*YFP* or $35S_{pro}$:*HBI1-YFP* and the $35S_{pro}$:*YFP*, and then normalized to that of the control gene *PP2A*. Three biological repeats were conducted.

Short-term nitrate induction assay of *HBI1* expression

The $HBI1_{pro}$:*LUC* transgenic line was grown on nitrogen-free medium for 5 days and then transferred to 10-mM KNO_3 plates containing 1-mM D-luciferin at different times; subsequently, fluorescence images were detected by Tanon 5200 fully automatic chemiluminescence image analysis system.

Measurements of ROS production

ROS was detected by H_2DCFDA, NBT, and 3,3′-diaminobenzidine tetrahydrochloride (DAB) staining. For H_2DCFDA staining, seedlings were incubated with 50-μM H_2DCFDA solution for 10 min in the dark and then washed with distilled water to remove excess dye. Examinations of fluorescence intensity were performed using a laser scanning confocal microscope (excitation, 488 nm; emission, 505–550 nm; Zeiss, LSM700). For NBT and DAB staining, seedlings were incubated with 1-mg·mL^{-1} NBT solution or 1-mg·mL^{-1} DAB solution for 2 h at room temperature. Samples were then immersed in 80% (v/v) ethanol for 10 min to terminate the staining before being photographed.

Subcellular localization assay

To analyze NLP7-YFP nuclear retention triggered by nitrate and H_2O_2 in Arabidopsis, seedlings of $35S_{pro}$:*NLP7-YFP* transgenic plants were grown on the medium with or without 10-mM KCl, 10-mM KNO_3, and/or different concentrations of H_2O_2 for 7 days. To analyze NLP6-YFP and NLP7-YFP nuclear retention triggered by nitrate and H_2O_2 in *N. benthamiana*, $35S_{pro}$:*NLP6-YFP* and $35S_{pro}$:*NLP7-YFP* construct were transformed into *Agrobacterium* strain GV3101, agrobacterium was diluted to a final concentration of OD_{600} = 0.4, and then injected into *N. benthamiana* leaves with a needle tube. The plants were scooped out from soil and grown on the nitrate-free medium for 2 days before transformation with *Agrobacterium* containing the $35S_{pro}$:*NLP7-YFP* construct. After 36 h, these plants were treated with 10-mM KCl, 10-mM KNO_3, and/or 0.5-mM H_2O_2 for 1 h. To analyze nitrate-induced nuclear localization of NLP7-YFP in *hbi-q* and *cat2 cat3* mutants. Seedlings of $35S_{pro}$:*NLP7-YFP*, $35S_{pro}$:*NLP7-YFP*/*hbi-q*, $35S_{pro}$:*NLP7-YFP*/*cat2 cat3*, $NLP7_{pro}$:*NLP7-YFP*, $35S_{pro}$:*NLP7-YFP*/$35S_{pro}$:*HBI1-Myc* were grown on medium containing 10-mM KCl or 10-mM KNO_3 for 7 days. The fluorescence of YFP in the leaves was imaged using a confocal laser scanning microscope (Zeiss, LSM700); excitation was set to 488 nm (YFP) and images at emissions 505–550 nm (YFP) were collected. Image J was used to quantitatively analyze the data; florescence intensity from at least 50 pavement cells was recorded.

Phos-tag sodium dodecyl sulphate–polyacrylamide gel electrophoresis assay

Transgenic plant *35Spro:NLP7-YFP* growing on medium with 10 mM KNO_3 for 5 days was transferred to nitrogen-free medium for 2 days, and then treated with 10-mM KCl, KNO_3 and/or 0.5-mM H_2O_2 for 0.5 h. Harvested seedlings were ground in liquid nitrogen, powder was suspended in 1 X sodium dodecyl sulphate–polyacrylamide gel electrophoresis (SDS–PAGE) sample buffer, and centrifuged at 13,523*g* for 10 min and the supernatant was used for Phos-tag SDS–PAGE analyses. Phos-Tag was purchased from FUJIFILM Wako Pure Chemical Corporation and used according to the manufacturer's protocol. Gels for Phos-tag SDS–PAGE consisted of a separating gel added 25-μM Phos-tag acrylamide, 100-μM $ZnCl_2$. The anti-YFP (TransGen Biotech, Cat: HT801, 1:5,000 dilution) and anti-actin (Invitrogen, Cat: MA1-744, 1:5,000 dilution) antibodies were used to detect NLP7-YFP and actin, respectively.

RNA-Seq

Wild-type Col-0 seedlings, *nlp7-1* and *hbi-q* mutants growing on medium with 7-mM KNO_3 for 7 days were transferred to nitrogen-free medium for 2 days then treated with 10-mM KNO_3 for 3 h. To analyze the effects of H_2O_2 on nitrate regulated gene expression, Col-0 seedlings growing on medium with 7-mM KNO_3 for 7 days were transferred to nitrogen-free medium for 2 days then treated with 10-mM KNO_3 with or without 0.5-mM H_2O_2 for 3 h or treated with H_2O_2 for 3 h. Total RNA was extracted with Trizaol RNA extraction kit (Transgene), and mRNA sequencing libraries construction and sequencing on the BGISEQ-500 platform were performed at Beijing Genomics Institute. The sequence reads were mapped to the Arabidopsis genome using HISAT and Bowtie2 software. The gene read counts were calculated by htseq-count with default parameters (Anders et al., 2015), and differential gene expression was analyzed using DESeq2 tool with the generalized linear model (Love et al., 2014). DEGs were defined by two-fold expression difference with false discovery rate <0.05.

Accession numbers

Sequence data from this article can be found in the Arabidopsis Genome Initiative or GenBank/EMBL databases under the following accession numbers: AT2G18300 (*HBI1*), AT4G36540 (*BEE2*), At1g59640 (*bHLH031*), At5g62610 (*bHLH079*), At1g18400 (*BEE1*), At4g34530 (*CIB1*), AT2G43060 (*IBH1*), AT4G24020 (*NLP7*), AT1G12110 (*NRT1.1*), AT1G08090 (*NRT2.1*), AT1G08100 (*NRT2.2*), AT1G77760 (*NIA1*), AT4G35090 (*CAT2*), AT1G20620 (*CAT3*), AT3G01190 (*PRX27*), AT1G14550 (*PRX5*), AT5G05340 (*PRX52*), AT3G03670 (*PRX28*), AT5G39580 (*PRX62*), AT1G03850 (*GRXS13*), *PP2A* (AT1G13320), and AT5G40850 (*UPM1*). All sequencing data that support the finding of this study have been deposited in the National Center for Biotechnology Information Gene Expression Omnibus (GEO) and are accessible through the GEO series accession number GSE174025.

Supplemental data

The following materials are available in the online version of this article.

Supplemental Figure S1. Nitrate increases the activity of *HBI1* at the transcriptional level (supports Figure 1).

Supplemental Figure S2. Nitrate induces the expression of several members of *HBI1* gene family (supports Figure 1).

Supplemental Figure S3. Mutation of *HBIs* reduces the nitrate-mediated plant growth and development (supports Figure 2).

Supplemental Figure S4. Mutations of *HBIs* reduces the nitrate sensitivity of shoot growth (supports Figure 2).

Supplemental Figure S5. NRT1.1 is required for HBI1-promoted shoot growth (supports Figure 2).

Supplemental Figure S6. HBI1 participates in the nitrate-regulated expression of some ROS-related Genes (supports Figure 3).

Supplemental Figure S7. Mutation in *HBIs* reduces the nitrate-promoted scavenging of ROS in plants (supports Figure 4).

Supplemental Figure S8. Catalase plays important roles in HBI1-induced ROS scavenging (supports Figure 5).

Supplemental Figure S9. CATs are required for HBI1-stimulated plant growth (supports Figure 5).

Supplemental Figure S10. H_2O_2 inhibits the nitrate-induce root growth in a dose-dependent manner (supports Figure 6).

Supplemental Figure S11. CATs are required for the nitrate-induced expression of downstream genes (supports Figure 6).

Supplemental Figure S12. RNA-Seq analyzed the effects of H_2O_2 and nitrate on the gene expression (supports Figure 6).

Supplemental Figure S13. GO analysis the H_2O_2 and nitrate co-regulated genes (supports Figure 6).

Supplemental Figure S14. H_2O_2 has no significant effects on the nitrate-induced phosphorylation of NLP7 (supports Figure 7).

Supplemental Figure S15. H_2O_2 reduces the nitrate-induced nuclear localization of NLP7-YFP in the *NLP7pro:NLP7-YFP* transgenic plants (supports Figure 7).

Supplemental Figure S16. LMB attenuates the H_2O_2-inhibited nuclear localization of NLP7-YFP (Supports Figure 7).

Supplemental Figure S17. H_2O_2 has no significant effects on the subcellular localization of HBI1-YFP (supports Figure 7).

Supplemental Figure S18. HBI1 Enhances the nitrate-induced nuclear localization of NLP7-YFP (supports Figure 7).

Supplemental Figure S19. H_2O_2 attenuates the nitrate-induced nuclear localization of NLP6 (supports Figure 7).

Supplemental Data Set S1. Nitrate-regulated genes in wild-type plants.

Supplemental Data Set S2. Nitrate-regulated genes in *hbi-q* mutant.

Supplemental Data Set S3. Nitrate-regulated genes in *nlp7-1* mutant.

Supplemental Data Set S4. Nitrate-regulated overlap genes in Col-0, *hbi-q*, and *nlp7-1* mutants.

Supplemental Data Set S5. Genes regulated by nitrate in the presence of H_2O_2.

Supplemental Data Set S6. H_2O_2-regulated genes in wild-type plants.

Supplemental Data Set S7. Oligo used in this study.

Supplemental Data Set S8. ANOVA analysis in this study.

Supplemental Data Set S9. Amino acid sequences used for generating phylogenetic tree.

Acknowledgments

We thank Haiyan Yu and Xiaomin Zhao from the Analysis and Testing Center of SKLMT (State Key Laboratory of Microbial Technology, Shandong University) for assistance with the laser scanning confocal microscopy.

Funding

This work was funded by the National Natural Science Foundation of China (grant no. 31970306, 32070210, and 31870262), by the Shandong Province Natural Science Foundation (grant no. ZR2019ZD16 and 2019LZGC-015), by the China Postdoctoral Science Foundation (grant no. 2017M612259, 2018T110684 and 2020M672047), and by the Shandong Province Postdoctoral Science Foundation (grant no. 11200078311023 and 61200070311209).

Conflict of interest statement. The authors declare no conflict of interest.

References

Alvarez JM, Riveras E, Vidal EA, Gras DE, Contreras-López O, Tamayo KP, Aceituno F, Gómez I, Ruffel S, Lejay L (2014) Systems approach identifies TGA 1 and TGA 4 transcription factors as important regulatory components of the nitrate response of Arabidopsis thaliana roots. Plant J **80**: 1–13

Alvarez JM, Schinke A-L, Brooks MD, Pasquino A, Leonelli L, Varala K, Safi A, Krouk G, Krapp A, Coruzzi GM (2020) Transient genome-wide interactions of the master transcription factor NLP7 initiate a rapid nitrogen-response cascade. Nat Commun **11**: 1157

Anders S, Pyl PT, Huber W (2015) HTSeq—a Python framework to work with high-throughput sequencing data. Bioinformatics **31**: 166–169

Araya T, Miyamoto M, Wibowo J, Suzuki A, Kojima S, Tsuchiya YN, Sawa S, Fukuda H, von Wirén N, Takahashi H (2014) CLE-CLAVATA1 peptide-receptor signaling module regulates the expansion of plant root systems in a nitrogen-dependent manner. Proc Natl Acad Sci USA **111**: 2029–2034

Bai M-Y, Fan M, Oh E, Wang Z-Y (2012) A triple helix-loop-helix/basic helix-loop-helix cascade controls cell elongation downstream of multiple hormonal and environmental signaling pathways in Arabidopsis. Plant Cell **24**: 4917–4929

Bellegarde F, Maghiaoui A, Boucherez J, Krouk G, Lejay L, Bach L, Gojon A, Martin A (2019) The chromatin factor HNI9 and ELONGATED HYPOCOTYL5 maintain ROS homeostasis under high nitrogen provision. Plant Physiol **180**: 582–592

Bielski BHJ, Shiue GG, Bajuk S (1980) Reduction of nitro blue tetrazolium by CO_2^- and O_2^- radicals. J Phys Chem **84**: 830–833

Cai H, Chai M, Chen F, Huang Y, Zhang M, He Q, Liu L, Yan M, Qin Y (2020) HBI1 acts downstream of ERECTA and SWR1 in regulating inflorescence architecture through the activation of the brassinosteroid and auxin signaling pathways. New Phytol **229**: 414–428

Chaiwanon J, Wang W, Zhu J-Y, Oh E, Wang Z-Y (2016) Information integration and communication in plant growth regulation. Cell **164**: 1257–1268

Chu X, Li M, Zhang S, Fan M, Han C, Xiang F, Li G, Wang Y, Xiang C-b, Wang J-G, et al. (2020). HBI1-TCP20 interaction positively regulates the CEPs-mediated systemic nitrate acquisition. J Integr Plant Biol. DOI: 10.1111/jipb.13035.

Crawford NM, Forde BG (2002) Molecular and developmental biology of inorganic nitrogen nutrition. Arabidopsis Book **1**: e0011–e0011

Drerup MM, Schlücking K, Hashimoto K, Manishankar P, Steinhorst L, Kuchitsu K, Kudla J (2013) The calcineurin B-like calcium sensors CBL1 and CBL9 together with their interacting protein kinase CIPK26 regulate the Arabidopsis NADPH oxidase RBOHF. Mol Plant **6**: 559–569

Fan M, Bai M-Y, Kim J-G, Wang T, Oh E, Chen L, Park CH, Son S-H, Kim S-K, Mudgett MB, et al. (2014). The bHLH transcription factor HBI1 mediates the trade-off between growth and pathogen-associated molecular pattern–triggered immunity in Arabidopsis. Plant Cell **26**: 828–841

Forde BG (2014) Nitrogen signalling pathways shaping root system architecture: an update. Curr Opin Plant Biol **21**: 30–36

Fredes I, Moreno S, Díaz FP, Gutiérrez RA (2019) Nitrate signaling and the control of Arabidopsis growth and development. Curr Opin Plant Biol **47**: 112–118

García-Santamarina S, Boronat S, Hidalgo E (2014) Reversible cysteine oxidation in hydrogen peroxide sensing and signal transduction. Biochemistry **53**: 2560–2580

Gras DE, Vidal EA, Undurraga SF, Riveras E, Moreno S, Dominguez-Figueroa J, Alabadi D, Blázquez MA, Medina J, Gutiérrez RA (2018) SMZ/SNZ and gibberellin signaling are required for nitrate-elicited delay of flowering time in Arabidopsis thaliana. J Exp Bot **69**: 619–631

Guan P, Ripoll J-J, Wang R, Vuong L, Bailey-Steinitz LJ, Ye D, Crawford NM (2017) Interacting TCP and NLP transcription factors control plant responses to nitrate availability. Proc Natl Acad Sci USA **114**: 2419–2424

Haasen D, Köhler C, Neuhaus G, Merkle T (1999) Nuclear export of proteins in plants: AtXPO1 is the export receptor for leucine-rich nuclear export signals in Arabidopsis thaliana. Plant J **20**: 695–705

Ho C-H, Lin S-H, Hu H-C, Tsay Y-F (2009) CHL1 functions as a nitrate sensor in plants. Cell **138**: 1184–1194

Hu B, Jiang Z, Wang W, Qiu Y, Zhang Z, Liu Y, Li A, Gao X, Liu L, Qian Y (2019) Nitrate–NRT1. 1B–SPX4 cascade integrates nitrogen and phosphorus signalling networks in plants. Nat Plants **5**: 401

Hu HC, Wang YY, Tsay YF (2009) AtCIPK8, a CBL-interacting protein kinase, regulates the low-affinity phase of the primary nitrate response. Plant J **57**: 264–278

Huang NC, Chiang CS, Crawford NM, Tsay YF (1996) CHL1 encodes a component of the low-affinity nitrate uptake system in Arabidopsis and shows cell type-specific expression in roots. Plant Cell **8**: 2183–2191.

Jung J-Y, Ahn JH, Schachtman DP (2018) CC-type glutaredoxins mediate plant response and signaling under nitrate starvation in Arabidopsis. BMC Plant Biol **18**: 281

Kobayashi M, Ohura I, Kawakita K, Yokota N, Fujiwara M, Shimamoto K, Doke N, Yoshioka H (2007) Calcium-dependent protein kinases regulate the production of reactive oxygen species by potato NADPH oxidase. Plant Cell **19**: 1065–1080

Landrein B, Formosa-Jordan P, Malivert A, Schuster C, Melnyk CW, Yang W, Turnbull C, Meyerowitz EM, Locke JCW, Jönsson H (2018) Nitrate modulates stem cell dynamics in Arabidopsis shoot meristems through cytokinins. Proc Natl Acad Sci USA **115**: 1382–1387

Li J, Liu J, Wang G, Cha J-Y, Li G, Chen S, Li Z, Guo J, Zhang C, Yang Y, et al. (2015). A chaperone function of NO CATALASE ACTIVITY1 is required to maintain catalase activity and for multiple stress responses in Arabidopsis. Plant Cell **27**: 908–925

Li L, Ye H, Guo H, Yin Y (2010) Arabidopsis IWS1 interacts with transcription factor BES1 and is involved in plant steroid hormone brassinosteroid regulated gene expression. Proc Natl Acad Sci USA **107**: 3918–3923

Lin Y-L, Tsay Y-F (2017) Influence of differing nitrate and nitrogen availability on flowering control in Arabidopsis. J Exp Bot **68**: 2603–2609

Liu K-h, Niu Y, Konishi M, Wu Y, Du H, Sun Chung H, Li L, Boudsocq M, McCormack M, Maekawa S, et al. (2017). Discovery of nitrate–CPK–NLP signalling in central nutrient–growth networks. Nature **545**: 311–316

Love MI, Huber W, Anders S (2014) Moderated estimation of fold change and dispersion for RNA-seq data with DESeq2. Genome Biol **15**: 550

Malinovsky FG, Batoux M, Schwessinger B, Youn JH, Stransfeld L, Win J, Kim S-K, Zipfel C (2014) Antagonistic regulation of growth and immunity by the Arabidopsis basic helix-loop-helix

transcription factor homolog of brassinosteroid enhanced expression2 interacting with increased leaf inclination1 binding bHLH1. Plant Physiol **164**: 1443–1455

Marchive C, Roudier F, Castaings L, Bréhaut V, Blondet E, Colot V, Meyer C, Krapp A (2013) Nuclear retention of the transcription factor NLP7 orchestrates the early response to nitrate in plants. Nat Commun **4**: 1713

Mittler R (2017) ROS are good. Trends Plant Sci **22**: 11–19

Moreno S, Canales J, Hong L, Robinson D, Roeder AHK, Gutiérrez RA (2020) Nitrate defines shoot size through compensatory roles for endoreplication and cell division in *Arabidopsis thaliana*. Curr Biol **30**: 1988–2000

Neuser J, Metzen CC, Dreyer BH, Feulner C, van Dongen JT, Schmidt RR, Schippers JHM (2019) HBI1 mediates the trade-off between growth and immunity through its impact on apoplastic ROS homeostasis. Cell Reports **28**: 1670–1678

O'Brien JA, Vega A, Bouguyon E, Krouk G, Gojon A, Coruzzi G, Gutiérrez RA (2016) Nitrate transport, sensing, and responses in plants. Mol Plant **9**: 837–856

Ogasawara Y, Kaya H, Hiraoka G, Yumoto F, Kimura S, Kadota Y, Hishinuma H, Senzaki E, Yamagoe S, Nagata K, et al. (2008). Synergistic activation of the Arabidopsis NADPH oxidase AtrbohD by Ca_2^+ and phosphorylation. J Biol Chem **283**: 8885–8892

Safi A, Medici A, Szponarski W, Marshall-Colon A, Ruffel S, Gaymard F, Coruzzi G, Lacombe B, Krouk G (2018) HRS1/HHOs GARP transcription factors and reactive oxygen species are regulators of Arabidopsis nitrogen starvation response. bioRxiv, **164277**.

Shin R, Berg RH, Schachtman DP (2005) Reactive oxygen species and root hairs in Arabidopsis root response to nitrogen, phosphorus and potassium deficiency. Plant Cell Physiol **46**: 1350–1357

Song Y, Li J, Liu M, Meng Z, Liu K, Sui N (2019) Nitrogen increases drought tolerance in maize seedlings. Funct Plant Biol **46**: 350–359

Stitt M (1999). Nitrate regulation of metabolism and growth. Curr Opin Plant Biol **2**: 178–186

Su T, Wang P, Li H, Zhao Y, Lu Y, Dai P, Ren T, Wang X, Li X, Shao Q, et al. (2018). The Arabidopsis catalase triple mutant reveals important roles of catalases and peroxisome-derived signaling in plant development. J Integr Plant Biol **60**: 591–607

Swift J, Alvarez JM, Araus V, Gutiérrez RA, Coruzzi GM (2020) Nutrient dose-responsive transcriptome changes driven by Michaelis–Menten kinetics underlie plant growth rates. Proc Natl Acad Sci USA **117**: 12531–12540

Tian Y, Fan M, Qin Z, Lv H, Wang M, Zhang Z, Zhou W, Zhao N, Li X, Han C, et al. (2018). Hydrogen peroxide positively regulates brassinosteroid signaling through oxidation of the BRASSINAZOLE-RESISTANT1 transcription factor. Nat Commun **9**: 1063

Trevisan S, Trentin AR, Ghisi R, Masi A, Quaggiotti S (2019) Nitrate affects transcriptional regulation of UPBEAT1 and ROS localisation in roots of Zea mays L. Physiol Plant **166**: 794–811

Vidal EA, Alvarez JM, Araus V, Riveras E, Brooks MD, Krouk G, Ruffel S, Lejay L, Crawford NM, Coruzzi GM, et al. (2020). Nitrate 2020: thirty years from transport to signaling networks. Plant Cell **32**: 2094–2119

Wang R, Xing X, Wang Y, Tran A, Crawford NM (2009) A genetic screen for nitrate regulatory mutants captures the nitrate transporter gene NRT1.1. Plant Physiol **151**: 472

Wang S, Li L, Xu P, Lian H, Wang W, Xu F, Mao Z, Zhang T, Yang H (2018a) CRY1 interacts directly with HBI1 to regulate its transcriptional activity and photomorphogenesis in Arabidopsis. J Exp Bot **69**: 3867–3881

Wang W, Bai M-Y, Wang Z-Y (2014) The brassinosteroid signaling network—a paradigm of signal integration. Curr Opin Plant Biol **21**: 147–153

Wang Y-Y, Cheng Y-H, Chen K-E, Tsay Y-F (2018b) Nitrate transport, signaling, and use efficiency. Annu Rev Plant Biol **69**: 85–122

Waszczak C, Carmody M, Kangasjärvi J (2018) Reactive oxygen species in plant signaling. Annu Rev Plant Biol **69**: 209–236

Wu, F.-H., Shen, S.-C., Lee, L.-Y., Lee, S.-H., Chan, M.-T., and Lin, C.-S. (2009). Tape-Arabidopsis Sandwich - a simpler Arabidopsis protoplast isolation method. Plant Methods **5**, 16.

Xu G, Fan X, Miller AJ (2012) Plant nitrogen assimilation and use efficiency. Annu Rev Plant Biol **63**: 153–182

Xu N, Wang R, Zhao L, Zhang C, Li Z, Lei Z, Liu F, Guan P, Chu Z, Crawford NM, Wang Y (2016) The Arabidopsis NRG2 protein mediates nitrate signaling and interacts with and regulates key nitrate regulators. Plant Cell **28**: 485–504

Yan D, Easwaran V, Chau V, Okamoto M, Ierullo M, Kimura M, Endo A, Yano R, Pasha A, Gong Y, et al. (2016). NIN-like protein 8 is a master regulator of nitrate-promoted seed germination in Arabidopsis. Nat Commun **7**: 13179

Yao N, Greenberg JT (2006) Arabidopsis ACCELERATED CELL DEATH2 modulates programmed cell death. Plant Cell **18**: 397–411

Yoo S-D, Cho Y-H, Sheen J (2007) Arabidopsis mesophyll protoplasts: a versatile cell system for transient gene expression analysis. Nat Protoc **2**: 1565–1572.